2013

Influence Of Implant Angulation On The Fracture Resistance Of Zirconia Abutments

Shreedevi Thulasidas
University of Alabama at Birmingham

INFLUENCE OF IMPLANT ANGULATION ON THE FRACTURE RESISTANCE OF ZIRCONIA ABUTMENTS

by

SHREEDEVI THULASIDAS

PERNG-RU LIU, COMMITTEE CHAIR
DANIEL GIVAN
JACK LEMONS
SANDRA O'NEAL
KEITH KINDERKNECHT
AMJAD JAVED

A THESIS

Submitted to the graduate faculty of the University of Alabama at Birmingham,
in partial fulfillment of the requirements for the degree of,
Master of Science

BIRMINGHAM, ALABAMA

2013

INFLUENCE OF IMPLANT ANGULATION ON THE FRACTURE RESISTANCE OF ZIRCONIA ABUTMENTS

SHREEDEVI THULASIDAS, D.D.S

MASTERS OF CLINICAL DENTISTRY

ABSTRACT

Zirconia-based implant abutments are widely used in prosthetic dentistry. Custom made abutments are utilized to correct for non-ideal implant positions and can successfully accommodate the morphologic requirements of the overlying crown. It was hypothesized that there will be difference in fracture strength and fracture mode of artificially aged zirconia implant abutments supported by implants at varying angulation, when load is applied to failure on overlying zirconia crowns. The implant-abutment-crown assemblies were subjected to steam autoclaving to induce some degree of phase transformation from tetragonal to weaker monoclinic form and to thermo-cycling to artificially age the samples. The effects of loading or occlusal forces applied to a model of implant-abutment-crown assembly with varying geometry of implant alignment was investigated in this study with customized zirconia implant abutments with internally hexed implant and overlying zirconia crowns loaded to fracture. Construct design and loading angulations were selected to simulate mouth conditions as closely as possible. Results showed that fracture strength of zirconia abutments was affected by the variation in the angulation of the implant. Aging did not seem to play a role in the fracture strength.

Key words: custom zirconia abutment, aging, angled zirconia abutment, fracture resistance, shorter internal connection, implant angulation

DEDICATION

I dedicate my thesis to God Almighty who gave me intellectual guidance, emotional support and physical strength at all the times so that I could stay focused in my work, be happy and impart happiness to people dear and near to me.

I also dedicate this thesis to my mother, Leelakumari Thankachy whose unconditional love and support has been my pillar of strength throughout my entire education and to my husband Dr. Thulasidas Chellppannair, who inspires me with his words and action and leads my pathway to reach my professional and personal goals of my life and finally to my little ones Sidharth and Sitara who give me immense love and joy that helped me find a balance between my personal life, patient care and research work.

ACKNOWLEDGEMENTS

I am grateful to Dr. Perng-Ru Liu for his continuous support for this project, from initial advice and contacts in the early stages of conceptual inception and through ongoing advice and encouragement to this day.

I would like to thank my mentors, Dr. Jack Lemons and Dr. Daniel Givan for their excellent mentorship, continuous guidance and lots of patience with me. They inspire me to think and answer my own questions. I would also like to thank my master's committee, especially Dr. Sandra O'Neal and Dr. Keith Kinderknecht for their support during the length of this investigation.

I would like to acknowledge Mr. Preston Beck for his guidance and physical support which helped me tremendously to successfully finish this project. I appreciate Dr. Lance Ramp for all the help with the statistical analysis and interpretation of results. I would like to say special thanks to Dr. Ramtin Sadid Zadeh who has been a good friend with whom I can share my happiness and frustrations.

I would like to thank American College of Prosthodontics Education Foundation for the financial support for this project. I would like to extend my special thanks to BioHorizons Inc., especially to Mr. Todd Strong for donating all the implants used in this study and Dr. Amjad Javed and Miss. Robbie Burrell for the administrative support.

TABLE OF CONTENTS

Page

LIST OF TABLES

LIST OF FIGURES

INTRODUCTION

Implant dentistry has evolved over the last three decades to stand out as a distinct branch of dentistry that offers patients with a unique opportunity to get their missing teeth replaced in a most predictable manner. The patient goes through an initial surgical phase where an endosseous implant is placed in its most ideal position followed by a restorative phase where implant gets loaded by an abutment and a crown.[1]

Replacement of teeth with an implant supported restoration in the anterior maxillary region requires a close working relationship between the surgeon and the restoring dentist in terms of comprehensive treatment planning and treatment execution. To mandate a predictable esthetic outcome and to ensure long term prosthesis success, surgery should be prosthetically driven and the use of surgical guide or prosthetic template becomes inevitable. Careful planning of the implant prosthesis in terms of crown contour and occlusal form should be done ahead of time to achieve ideal implant location. The use of a template facilitates implant placement in a prosthetically oriented position that is considered to be the ideal implant position. An ideal implant position optimizes biological and mechanical factors that contribute to the longevity of the implant-abutment-crown assembly and enables the clinician to deliver the implant restoration with the best possible prognosis and esthetics.

The long-term prognosis of the implant-prosthesis is of great concern to the clinician. The overall pre-prosthetic loss rate is lower than the failure rate after prosthetic

treatment.[2] Biomechanical factors play a major role in implant success or failure.[3,4,5,6] The application of occlusal forces induces stresses and strains within the implant-prosthesis complex and also affects the bone remodeling process around implants.[3,7,8] Various studies have stressed the importance of axial loading of implants to minimize the problems associated with non-axial loading.[9] Non-axial loading has been related to marginal bone loss, failure of osseointegration, failure of the implant and / or the prosthetic superstructure components, and, if connected to natural teeth, failure of the cement seal on the natural tooth.[10] But in cases where esthetics requires tooth overlap as in maxillary anterior region, off-axis loading of the implant becomes unavoidable.[11]

In the anterior maxillary segment, esthetics and emergence profile of the remaining dentition are the important parameters in determining the ideal implant position and the angulation. Error in placement of dental implants is always a possibility whenever prosthetic template is not utilized or in cases of severe resorption of the alveolar ridge following tooth extraction resulting in inadequate bone for ideal implant placement.[12] Studies such as the ten year retrospective investigation by Campelo & Camaro report that the level of operator experience has significant influence on the treatment outcome.[13] These scenarios can possibly create situations where the implant has not been placed in a prosthetically driven position causing the emergence angle of implant from the bone to be different from the emergence angle of the implant crown. The emergence angle of the implant crown is dictated by the emergence profile of the adjacent teeth. This mismatch is compensated by the use of angled stock abutments that needs some degree of adjustment or by custom milled abutments that can accommodate the emergence angulation of the implant crown.

This mismatch can also pose esthetics challenges to the clinician while restoring the implant crown. When the implant is placed in an ideal position, the restoring dentist should be able to create an implant restoration that emerges from the soft tissue scaffold to create an illusion of a natural tooth.[14] An implant placed too far buccally often results in a dehiscence of the buccal cortical plate and has a high potential for gingival recession.[15] In addition, this placement vastly complicates the restoration of the implant.[15] On the other hand, an implant placed too far to the palatal often requires a ridge-lap restoration that is both unhygienic and un-esthetic.[16]

The following clinical presentation is a typical example of non-ideal implant placement. The patient presented with an implant placed at # 8 tooth position where the emergence angle of the implant is relatively facial to the emergence profile of the adjacent teeth (Figure 1, 2). The Cone Beam Computerized Tomography (CBCT) evaluation of the implant site revealed the angulation mismatch to be close to 20 degrees. The gingival asymmetry is quite obvious (Figure 3) and it cannot be corrected even with custom abutment.

Figure.1. Emergence of implant from soft tissue at #8 tooth position

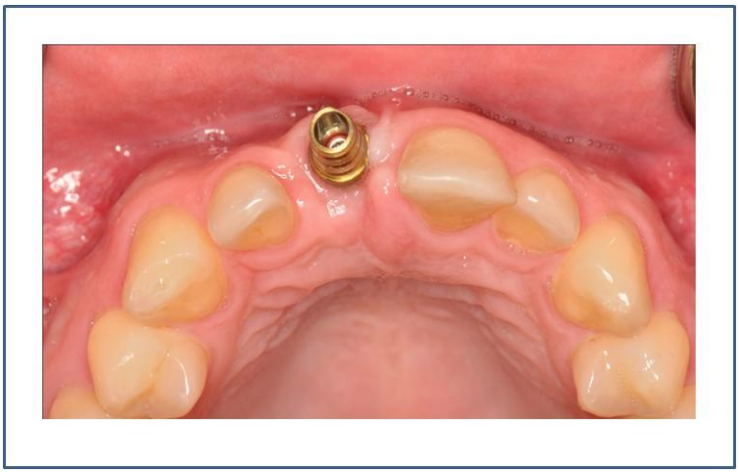

Figure.2. Facial placement of the implant

Figure.3. Gingival recession at the implant site

Current state of the art in implant prosthodontics in the esthetic zone is to employ all-ceramic crowns with all-ceramic abutments to optimize the esthetics of anterior tooth replacements. Highly esthetic implant restorations demands strong, tooth colored, tissue-compatible custom made abutments. Densely sintered, yttrium stabilized zirconia (Y-TZP) abutments has gained popularity as an esthetic abutment due to its high strength, white color and biocompatibility. Custom-made zirconia abutment can accommodate non-ideal implant placement where utilization of pre-fabricated component cannot provide the required support for the morphologic features of the overlying crown. But being a ceramic material with its inherent brittleness, zirconia abutment is sensitive to tensile forces and breakage.

The following is an example of zirconia abutment breakage after two years of use in-vivo (Figure 4, 5). The patient presented with a “spinning crown” at tooth #10 location. Clinical examination revealed that the abutment screw was loose and the hex of the zirconia abutment has been broken.

Figure.4. Clinical presentation of the crown

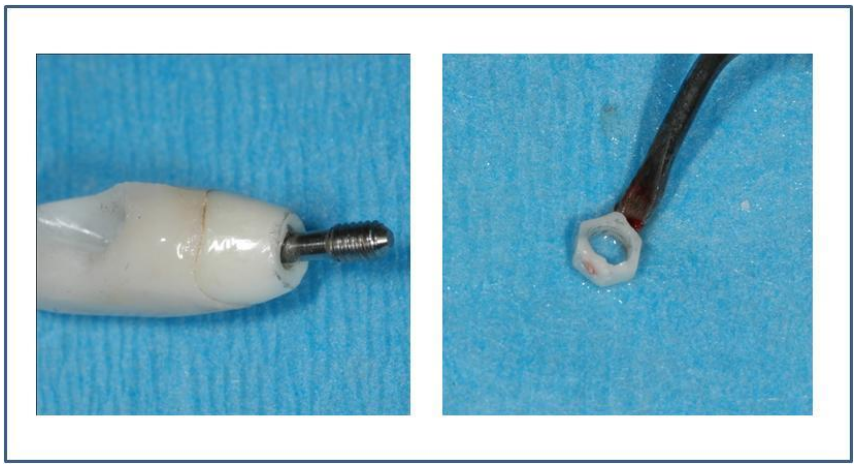

Figure.5. Zirconia abutment broken at the hex portion that engages the implant body

Various in-vitro studies have been performed to evaluate the fracture resistance of zirconia abutments under varying simulated clinical conditions.[17,18,19,20,21,22] In general, data on the fracture strength of zirconia abutments are difficult to compare between studies because of the difference in the study design. These studies demonstrated that fracture of the zirconia abutment occurred at the cervical portion of the abutment, near the screw and platform of the implant. This area has been presumed to be an area of the highest torque and stress concentrations due to the levering effect. Various factors that can modify the fracture load of zirconia abutment include type of implant-abutment connection, angle of loading, point of loading, abutment design whether it is straight or angulated, one piece or a two piece abutment design with a metallic secondary component, type of aging treatment etc.

Despite a high elastic modulus of 215 GPa and flexural strength of 1000 MPa that exceeded those of many metallic alloys, zirconia cannot be used in thin sections due to its characteristic brittleness.[23] Aboushelib & Salameh [24] retrieved five clinically fractured zirconia abutments, performed fractographic analysis and attributed two of the sample

failures to over reduction of the axial walls and concluded that in order for the zirconia abutment to resist the applied functional loads, the minimal wall thickness should not be reduced beyond 0.5 mm to 0.7 mm. Other studies investigated the influence of implant abutment angulation on the fracture resistance of overlaying zirconia crown and found that the implant angulation of 30 degree significantly reduced the fracture resistance of overlaying CAM milled zirconia crown.[25] Reducing the core thickness of the overlying crown from 0.8mm to 0.4mm did not affect the fracture resistance of the overlying crown.[25] It was also reported in the literature that when two piece zirconia abutment that uses a secondary metallic component were used with implants with internal connection, it outperformed one piece zirconia abutment in the fracture strength.[18]

There appears to be a correlation between measured fractured load and the type of implant abutment connection.[26] Internal connection of abutments tends to be beneficial both in the laboratory and in the clinical studies.[26] In laboratory studies, the internal conical connection was demonstrated to exhibit significantly higher strength than the external hexagonal connection due to a higher resistance to bending.[26] Internal connection has also been associated with a more favorable load distribution in the connection area.[27] A finite element analysis demonstrated high tensile stresses in the abutment screw threads upon lateral loading of an externally connected abutment (butt joint design), whereas with a tapered internal connection, lateral loading was taken up by the taper, thus protecting the thread portion of the abutment from load transfer.[28] The degree of abutment fracture protection that a short internal connection offers could be different from that offered by a longer internal connection. This area needs further investigation.

Dentistry uses the tetragonal form of zirconia (Y-TZP) that is partially stabilized by the yttria, which helps to retain its physical properties at room temperature. The Y-TZP owes its high strength and toughness to its meta-stability: it is toughened as it undergoes stress induced *tetragonal→monoclinic (t-m)* martensitic transformation at room temperature.[29] This phase transformation induces compressive stresses and micro-cracks around the transformed particles, which effectively oppose the opening of cracks and increase the resistance to crack propagation.[29] This property that is unique to zirconia is called transformation toughening.[29]

The *(t-m)* phase transformation can also occur at low temperatures, especially in the presence of water. This is commonly known as aging or low-temperature degradation (LTD).[30] The main features of this so-called low-temperature degradation (LTD) are the following:[34]

i. transformation proceeds most rapidly at temperatures of 200–300°C and is time dependent
ii. water or water vapor enhances the transformation
iii. transformation proceeds from the surface to the bulk of the zirconia materials
iv. higher stabilizing content or finer grain size increases the resistance to transformation

Aging occurs by a nucleation and growth process of monoclinic nuclei which initiates from isolated surface grains, gradually spreads along the surface, and proceeds into the bulk, resulting in surface roughening and reductions in strength, toughness, and density.[31,32,33] Since the LTD induced *(t-m)* transformation in Y-TZP is thermally

activated and is accelerated by the presence of water, steam autoclave treatments at elevated temperatures can effectively induce phase transformation and can be considered as an accelerated form of aging. Since the thermal activation energy required for this phase transformation is ~106 kJ/ mol, it is estimated that 1 hour of steam autoclave treatment at 122°C under 2 bars has the same effect as 1 yr *in vivo.* [34]

Custom abutments are produced by CAD-CAM milling of the pre-sintered blocks and the subsequent sintering process partially heals the micro-cracks originating from the milling and eliminates voids and flaws.[35] Sintering facilitated the *monoclinic → tetragonal (m-t)* phase transformation and relieved surface compressive stresses derived from the CAD/CAM milling process.[35] Other studies that used SEM observation also demonstrated that the surface and subsurface micro-cracks are not fully healed by the final sintering process.[36] The rough surfaces, which consist of micro-cracks without the presence of any compressive stresses, eventually lead to increased low-temperature degradation of CAD/CAM Y-TZP surfaces.[36] It has been well-documented that surface compressive stresses suppress the LTD process[37] while micro-cracks facilitate the LTD process by providing passage for water.[38]

The oral cavity is a dynamic environment where force factors, temperature and chemistry of saliva are constantly changing, all of which may negatively impact the mechanical properties of zirconia abutment.[29]

Many studies have been conducted to test the mean fracture load of zirconia abutments under varying loading conditions and angulations, none of the studies done so far have investigated the effect of varied implant angulation on the fracture resistance of

zirconia abutments that has been artificially aged to simulate the structural changes occurring within zirconia abutment in-vivo. It will be relevant to clinicians if researchers can investigate the effects of aging on the fracture strength of straight and angulated zirconia abutments to simulate clinical conditions.

The outcomes from this research should be clinically relevant when considering implant prosthetic solutions for patients with deficient bone or unwanted surgical outcomes, both of which require angled abutments. The CAD/CAM applications for implant abutments provide the clinician with opportunities to customize abutments at angles much greater than those found in most commercially available pre-fabricated systems. However, modifying the zirconia abutment design to accommodate the emergence angle of the overlying crown may affect the stress bearing capacity and fracture resistance of the customized abutment. This coupled with the naturally occurring phenomenon of aging from low temperature degradation further creates the possibility of material degradation and failure with time. Greater understanding of the effects of implant angulation on zirconia abutments and aging may lend to the improvement of clinical protocols and may possibly limit potential failures of implant prosthetics.

OBJECTIVES

In this study, the effects of occlusal force will be investigated on artificially aged zirconia abutments when considering different orientations of the supporting implant.

Null Hypothesis 1

There is no difference in fracture strength of zirconia abutments when a load is applied to failure on crowns supported with implants at varying angulation.

Specific Aim 1

A model of implant-abutment-crown assembly will be designed with implants positioned at 0°, 20 degree facial (20F) and 20 degree lingual (20L) positions. Variation in angulation of implant is compensated with varied abutment design so that it will fit a crown with the same outside and inside dimensions. Load will be applied to failure at a constant cross-head speed capturing force versus time data. Differences between groups will be evaluated with two way ANOVA with Tukey's multiple comparisons to reject or fail to reject the hypothesis.

Null Hypothesis 2

There is no difference in fracture strength of zirconia abutments when subjected to thermal degradation and thermocycling.

Specific Aim 2

Half of the samples from every group, namely the 0, 20F and 20L will be subjected to thermal degradation and thermocycling. Since the *(t-m)* phase transformation

in Y-TZP is thermally activated and is accelerated by the presence of water, steam autoclave treatments at elevated temperatures can effectively induce phase transformation. Differences between groups will be evaluated with two way ANOVA with Tukey's multiple comparisons to reject or fail to reject the hypothesis.

Null Hypothesis 3

There is no difference in fracture mode of zirconia abutments when load is applied to failure on crowns supported with implants at varying angulation.

Specific Aim 3

Specimens from each group will be examined under light microscopy for general mode of fracture from initiation, propagation, and catastrophic failure to reject or fail to reject the hypothesis.

MATERIALS AND METHODS

The study design is given in table 1.

Table 1. Study design

group	no. of samples	Implant	Implant angle	Abutment	Treatment
1	10	BH 4.6x15	0	custom milled	no treatment
2	10	BH 4.6x15	20F	custom milled	no treatment
3	10	BH 4.6x15	20L	custom milled	no treatment
4	10	BH 4.6x15	0	custom milled	steam autoclave & thermocycling
5	10	BH 4.6x15	20F	custom milled	steam autoclave & thermocycling
6	10	BH 4.6x15	20L	custom milled	steam autoclave & thermocycling

BH 4.6x15 - BioHorizons implant (4.6x15 mm, tapered internal, catalog # TLXP4615)

Testing Model

A model of an implant-abutment-crown is constructed to test the hypotheses. Zirconia abutments and zirconia crowns are CAD-CAM milled. Implants angulations are varied at 0 degree, 20 degree to the facial and 20 degree to the lingual. The zirconia abutments are customized by CAD-CAM technology to compensate for the varying implant angulation so that it can fit the constant crown contours. The digital work flow and integration in the fabrication of the test specimen is shown in Figure 6. Details of the design and fabrication is explained below.

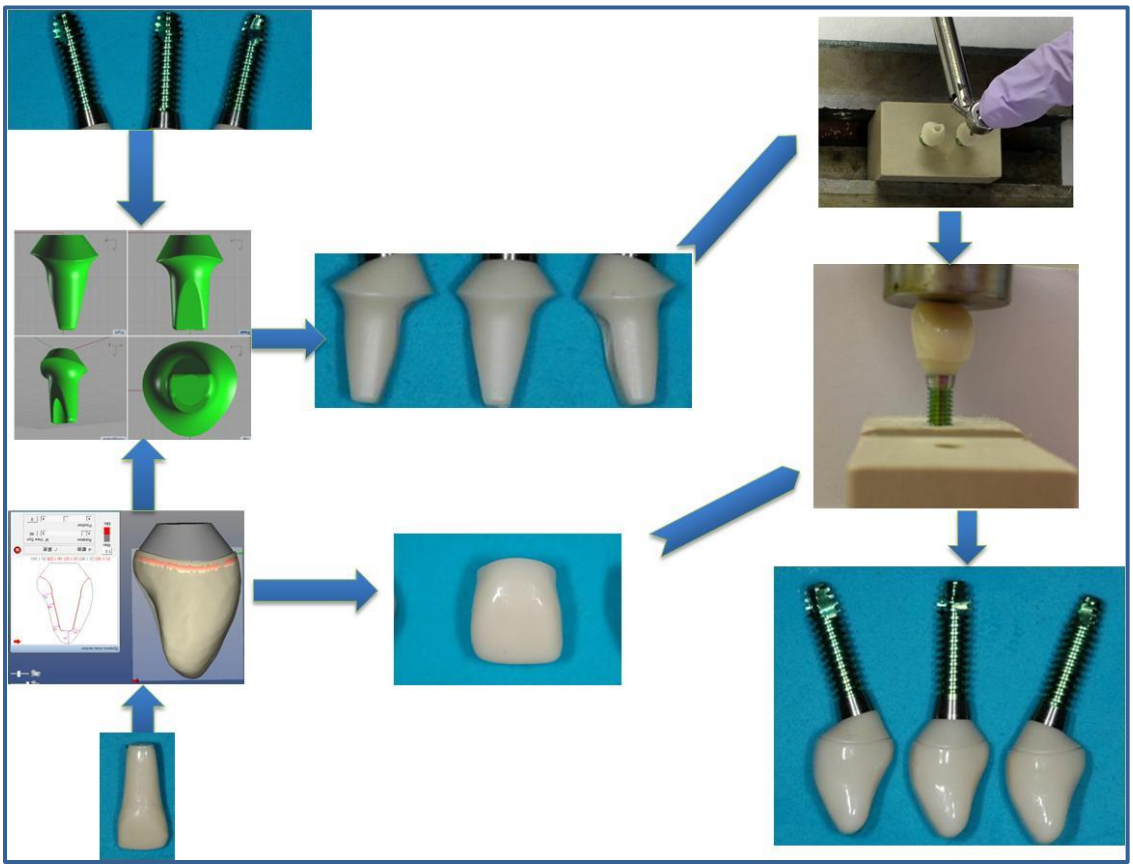

Figure.6. Digital work flow and integration

A typodont tooth # 8 (Columbia Dentoform Corporation, Long Island City, NY) was scanned to facilitate computer-aided design for the zirconia crowns used in this study (Figure 7). This was done because the typodont tooth closely resembles the average dimensions of a central incisor. All the crowns were CAD-CAM generated to have the same emergence profile, same marginal contours and external and internal morphology to precisely fit all the abutments in the three different angulation groups in the same manner. The crowns used in this study were monolithic and glazed. For the crown, high translucent zirconia blanks (HT) were used and for glazing e.max ceram was used. The sintering temperature used was 1530 degree C. The sintering time was 3 hours at a

heating rate of 16.8 ^{0}C per minute. Fabrication of the crown was accomplished with the help of CAD-CAM technology. The crown dimensions were kept as a constant factor in all dimensions on all restorations. The monolithic zirconia crown was chosen to avoid veneering porcelain fracture during the loading procedure. The zirconia custom abutments were made from high strength zirconia blanks. The sintering temperature used was 1530 degree C. The sintering time was 2 hours at a heating rate of 16.8 ^{0}C per minute. No other special treatment was done after sintering. The properties of the zirconia material are listed in Appendix A.

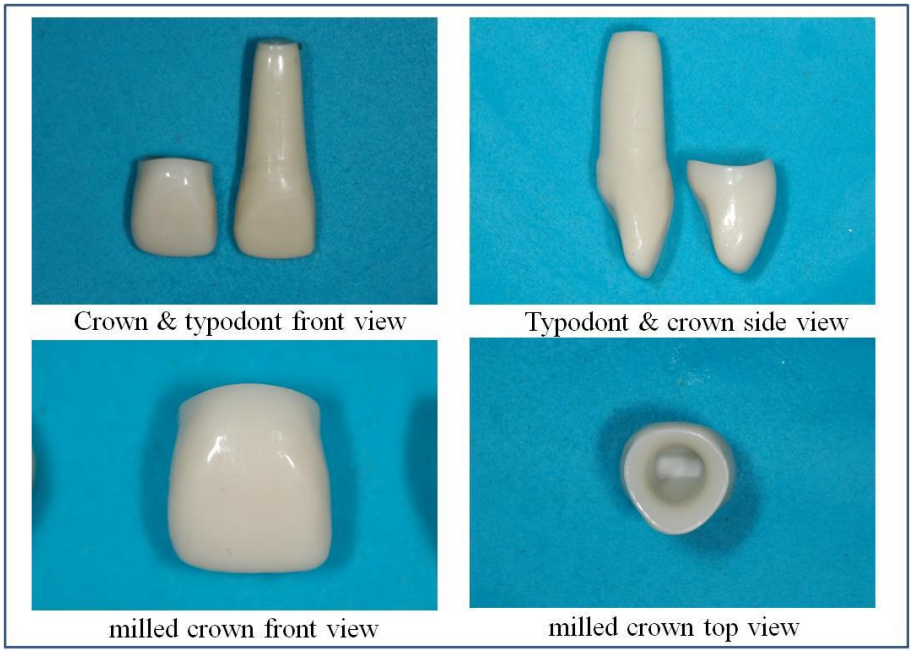

Figure 7. Typodont tooth #8 and CAD milled crown

The zirconia abutment was designed to fit the constant zirconia crown contours (Figure 8) and also to fit the internal connection of BioHorizons implant (4.6x15 mm, tapered internal, catalog # TLXP4615, BioHorizons, Inc., Birmingham, AL) at three different angulation namely 0 degree (Figure 9), 20 degrees to the facial (Figure 10) and 20 degrees to the lingual (Figure 11). The marginal configuration of all the abutments

was kept as a constant factor so the abutments from all the groups precisely fit the crown and vice versa.

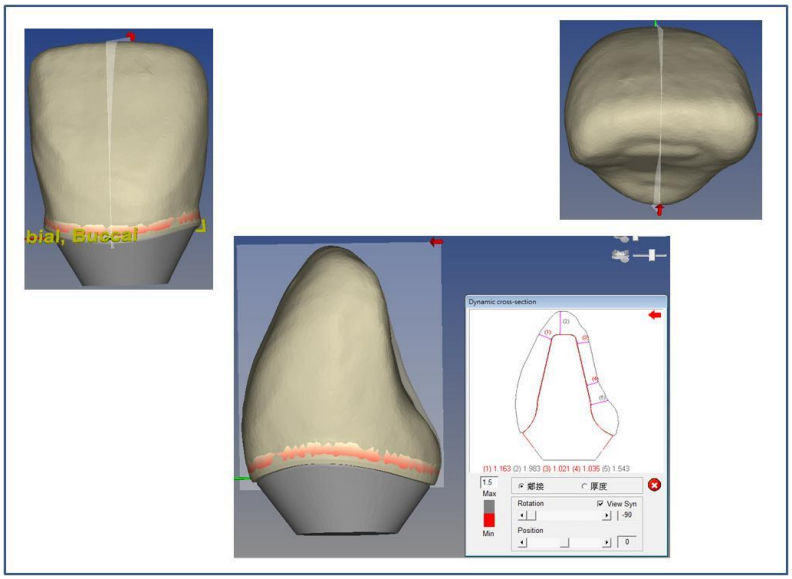

Figure 8. CAD design for the zirconia abutment

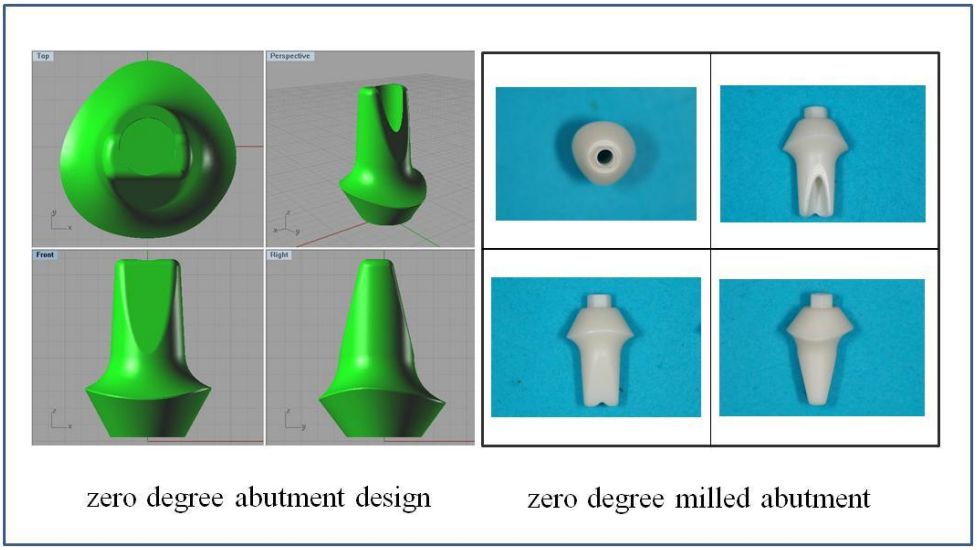

Figure 9. Zero degree abutment design and CAD milled abutment

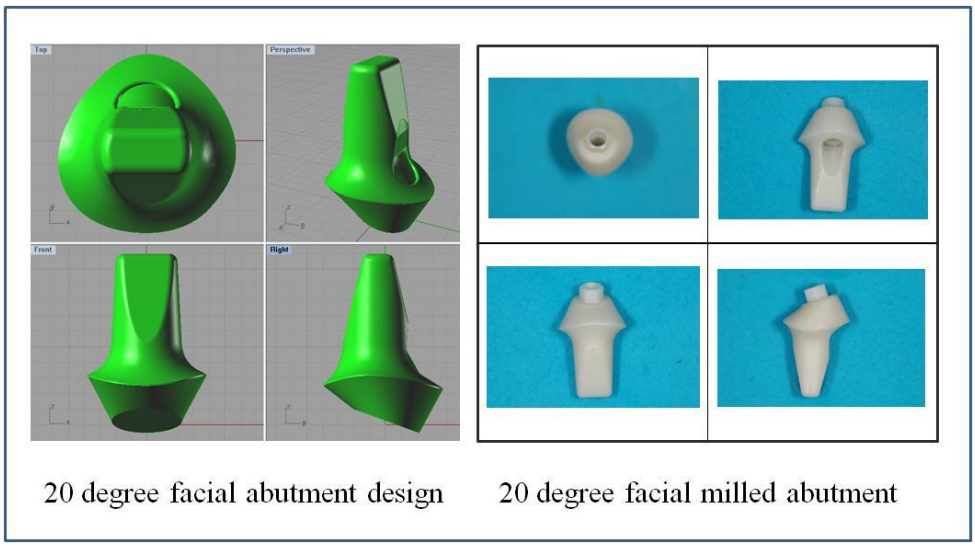

Figure 10. 20 degree facial abutment design and CAD milled abutment

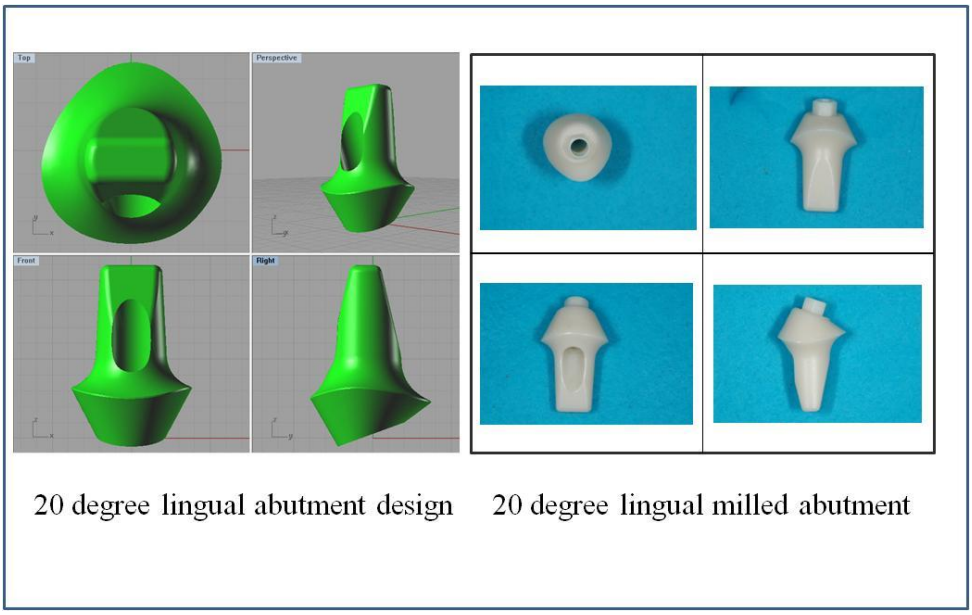

Figure 11. 20 degree lingual abutment design and CAD milled abutment

The angle correction is demonstrated in Figure 12. The angle correction caused the abutment in every group to have a varied screw hole location and different material thickness around the screw hole. The angle corrected abutments in every group had unique emergence profile because the gingival contours was kept as a constant factor.

Varied emergence profile caused the abutments to have different height occluso-gingivally in the facial and lingual dimension. This is demonstrated in the photographs in Figure 13.

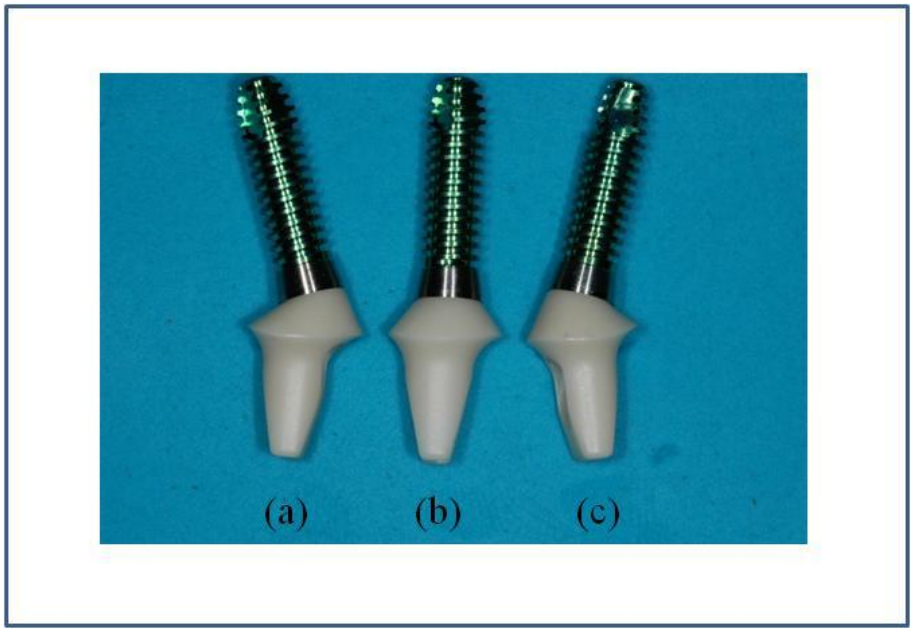

Figure 12. Customized angle corrected abutment designed to fit the constant crown contour (a) 20 degree facial (b) 0 degree (c) 20 degree lingual

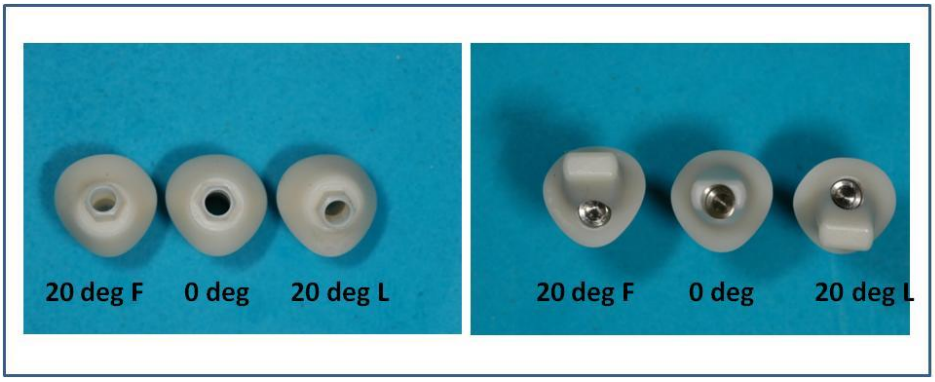

Figure 13. Screw hole locations on abutment samples for the three groups

A total of 60 zirconia custom abutments and 60 zirconia crowns were produced by TurboDent System (Pou Yu Biotechnology Co., Ltd., No. 6 Fugong Rd., Fusing

Township, Changhua County 506, Taiwan). The properties of the zirconia material used in the crown and abutments are listed in Appendix A.

A sketch showing the zero degree abutment dimensions from the mesial, distal, facial and lingual aspect is shown in Figure 14. These measurements were made for all 20 samples using a digital caliper and the data is given in Appendix B. In the 0 degree group, the screw hole location is in the middle and the mean values for M=2.33 mm, D=2.31 mm, F=2.77 mm, L=2.53 mm (Figure 15).

A sketch showing the 20F abutment dimensions from the mesial, distal, facial and lingual aspect is shown in Figure 16. The data for the 20 samples is given in Appendix C. In the 20 B group, the screw hole location is in the lingual side and the mean values for M=3.43 mm, D=3.47 mm, F=3.58 mm, L=1.46 mm (Figure 17).

Similarly, the sketch showing the 20L abutment dimensions from the mesial, distal, facial and lingual aspect is shown in Figure 18. The data for the 20 samples is given in Appendix D. In the 20 L group, the screw hole location is in the facial side and the mean values for M=2.56 mm, D=2.59 mm, F=1.57 mm, L=2.71 mm (Figure 19).

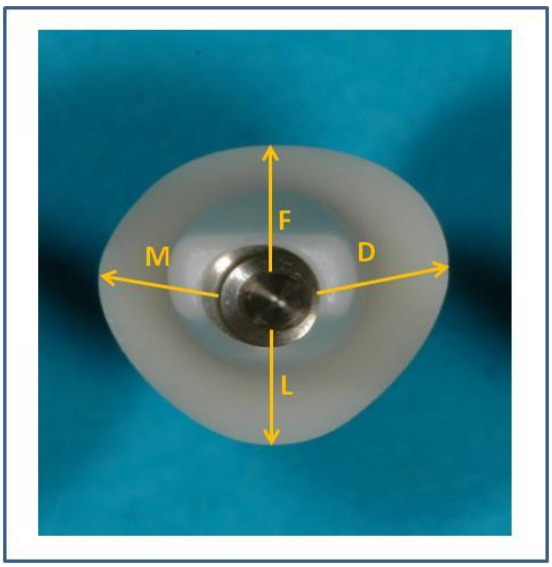

Figure 14. Sketch showing the zero degree abutment dimensions (M-Mesial, D-Distal, F- facial, L-Lingual)

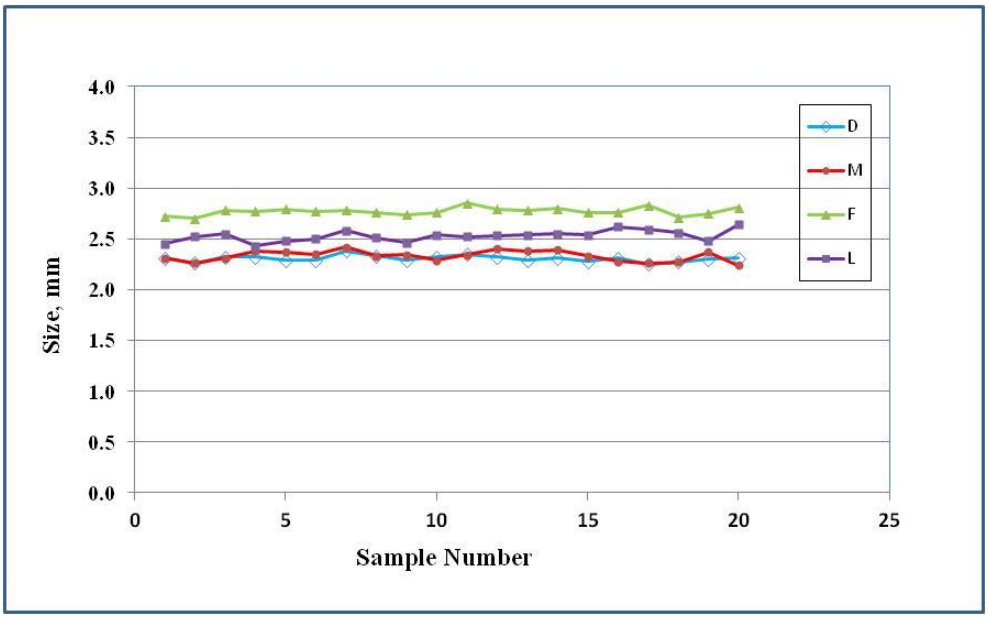

Figure 15. Variation in the zero degree abutment dimensions

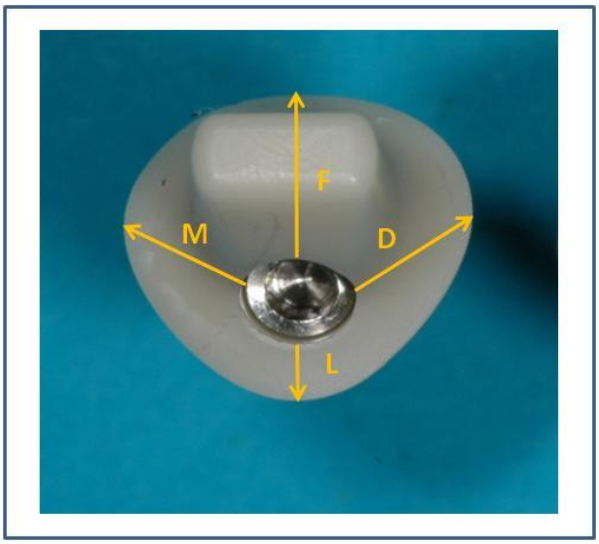

Figure 16. Sketch showing the 20 degree facial abutment dimensions (M-Mesial, D-Distal, F-Facial, L-Lingual)

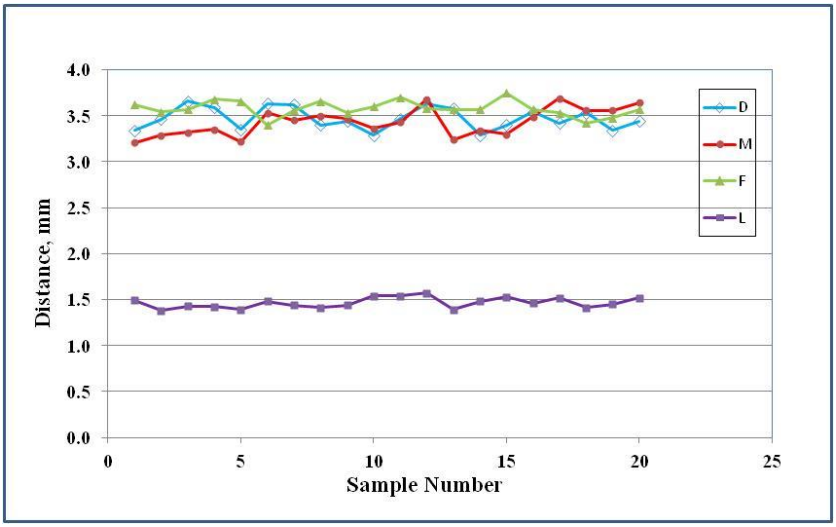

Figure 17. Variation in the 20 degree facial abutment dimensions

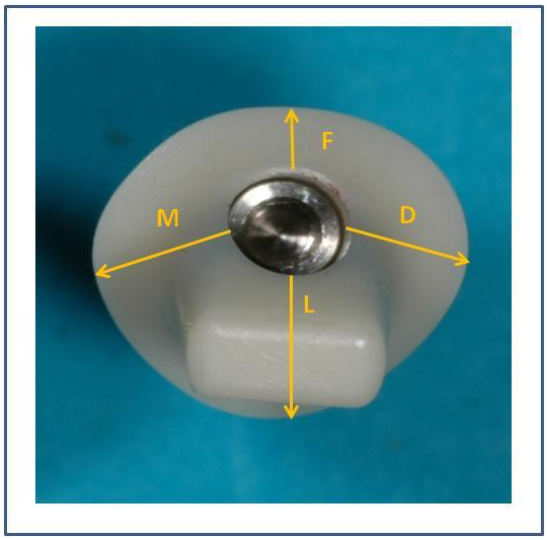

Figure 18. Sketch showig the 20 degree lingual abutment dimensions (M-Mesial, D-Distal, F-Facial, L-Lingual)

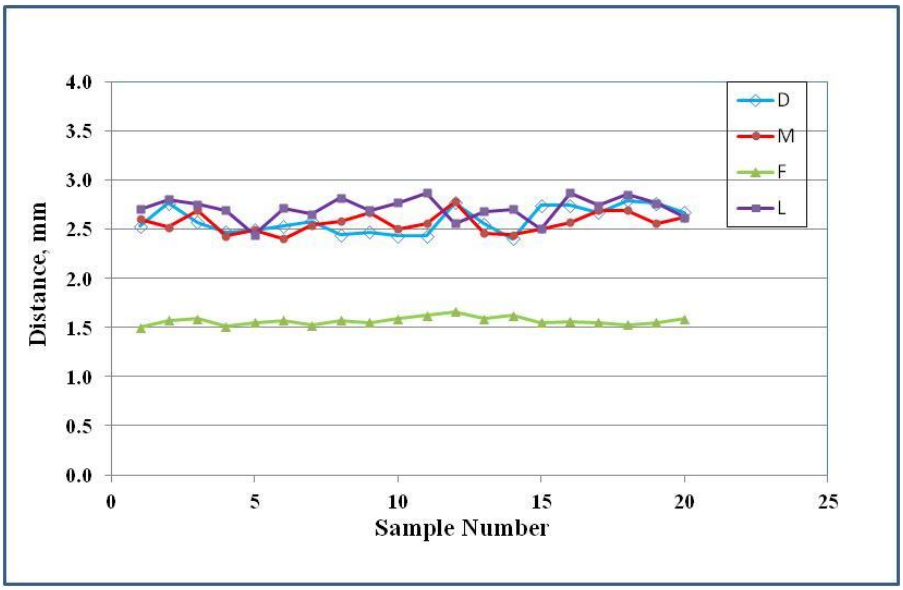

Figure 19. Variation in the 20 degree lingual abutment dimensions

Implant System

The implants used in this study were donated by BioHorizons, Inc (4.6 x15 mm, Figure 20). This implant has been chosen because this is the dimension most commonly used to replace a central incisor.

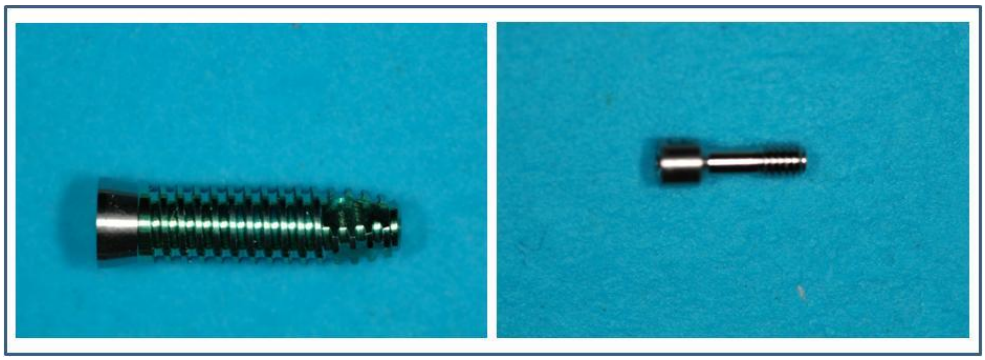

Figure 20. BioHorizons 4.6x15 mm tapered internal implant with screw

Specimen Fabrication

Specimens used in this study consisted of implant-abutment-crown assemblies mounted in a specimen holder made of a square aluminum tube with an internal cross section of 32x32mm, wall thickness of 3 mm and a depth of 25 mm. The details of specimen fabrication are explained below and it is comprised of the following steps:

1. Mounting Jig Fabrication
2. Torquing the Abutment on the Implant
3. Cementation of Zirconia Crowns on the Abutment
4. Steam Autoclaving and ThermoCycling of the Assembled Samples

5. Mounting the Samples in the Specimen Holder

Each of these steps is discussed in detail with aid of photographs.

1. Mounting Jig Fabrication

The purpose of the mounting jig is to help mount all the samples in a consistent and predictable manner. Essentially the outer contour of the crown, particularly the emergence profile is captured in the mounting jig (Figure 21). A surveyor table with a leveling gauge was used to accurately align the parts and pieces used for the fabrication of mounting jig. The photograph of the mounting jig is shown in Figure 22.

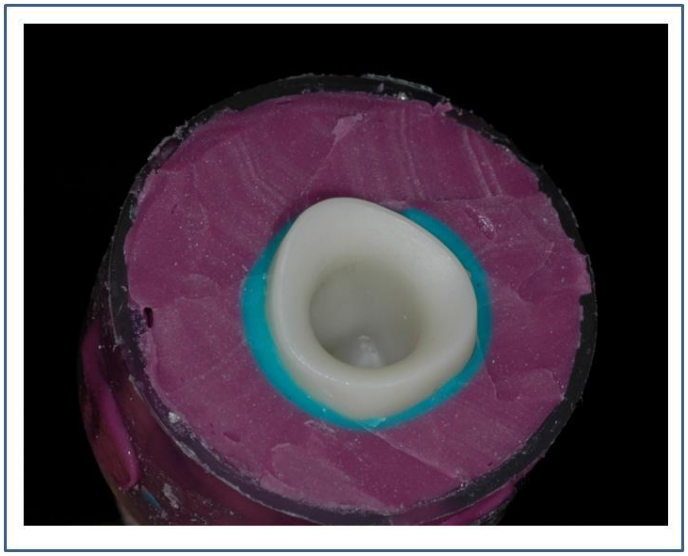

Figure 21. Mounting Jig with zirconia crown

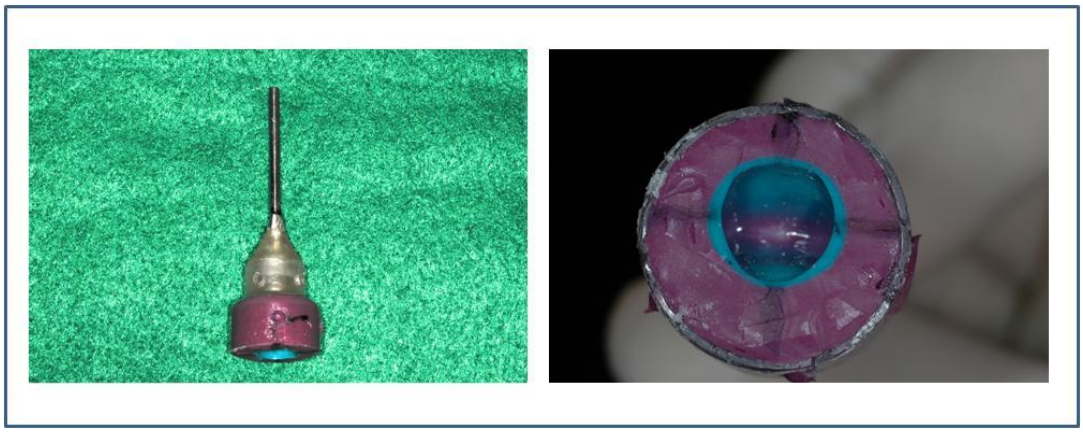

Figure 22. Mounting Jig

In the process of making the mounting jig, the zero degree abutment with the crown was used to capture the emergence profile of the crown because the zero degree abutment is the control sample. Additionally the ease of keeping the zero degree abutment straight with the analyzing rod in a surveyor gave excellent reproducible results. The implant-abutment assembly was connected to the analyzing rod which ensured the vertical position of the implant-abutment assembly in relation to the surveyor table. The surveyor table was maintained in the horizontal position with level gauges (Figure 23).

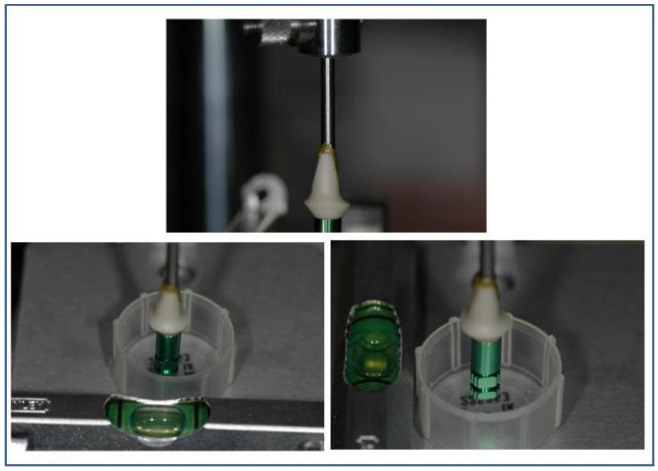

Figure 23. Vertical alignment of zero degree abutment

At this point, the vertical position of the implant-abutment assembly was captured with Poly methyl methacrylate (PMMA) (Orthodontic resin, Lang Dental Manufacturing Co Inc., Wheeling, IL) in a small flat reservoir placed on the horizontal table (Figure 24). This ensured 90 degree alignment of the abutment-implant assembly with respect to the surveyor table.

At this point the crown was secured to the implant-abutment assembly and the external crown contour was captured using PVS monophase impression material (Aquasil from Dentsply International, York, PA) in a small rigid plastic cup, which was kept in a vertical position with the help of the analyzing rod in a surveyor (Figure 25). The monophase impression material was selected as it has the right amount of resiliency and rigidity and provided the flexibility to use it multiple times without distortion. This finished the mounting jig fabrication phase.

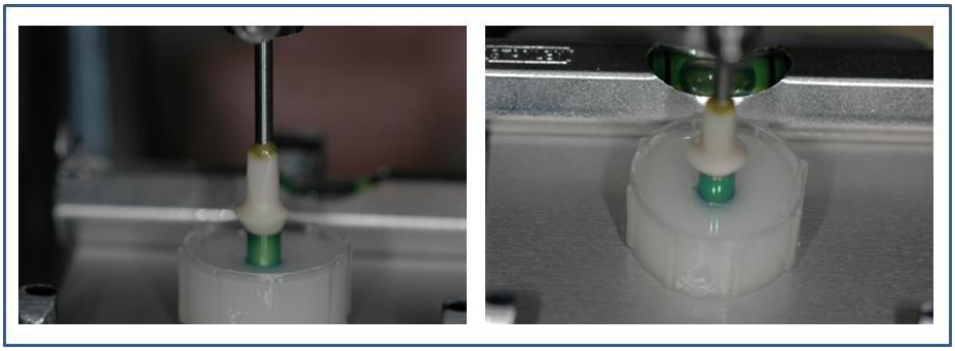

Figure 24. Verticality of Implant-abutment assembly is captured in PMMA

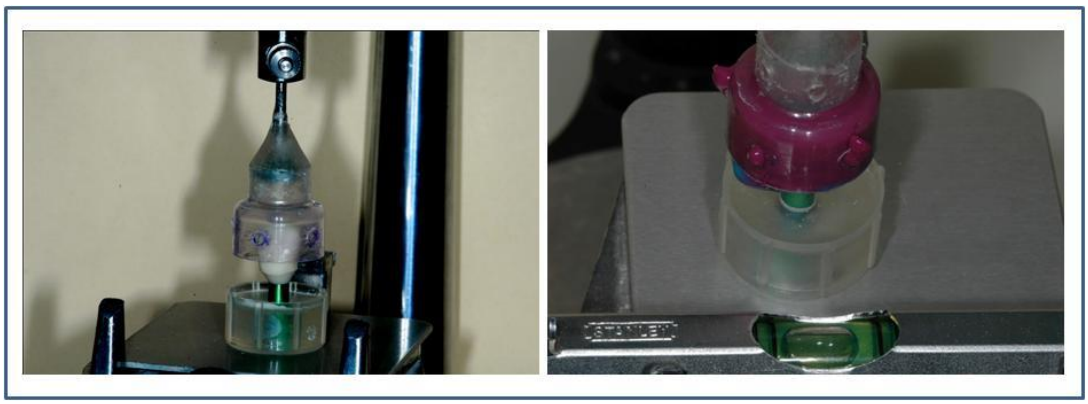

Figure 25. External crown contour is captured with PVS

Since the internal and external aspect of all the crowns in this study was kept as a constant factor, the abutments from all the three groups fit the crown in the same manner. Thus once the implant-abutment-crown assembly from a particular group was fitted to the mounting jig, it automatically aligned the implant to its predetermined angulation. The self-alignment of the implant-abutment-crown assembly is depicted in Figure 6.

2. *Torquing the Abutment in to the Implant*

The implant manufacture's recommended torque force of 30N-cm was applied while torquing the abutment into the fixture. The implant was secured in a custom torquing device made out of PolyEtherEther Ketone (PEEK) material (Figure 26) in which the implant threads are predrilled to facilitate subsequent implant placement. To ensure the execution of adequate torque, a torquing wrench from the implant manufacturer (BioHorizons) was used.

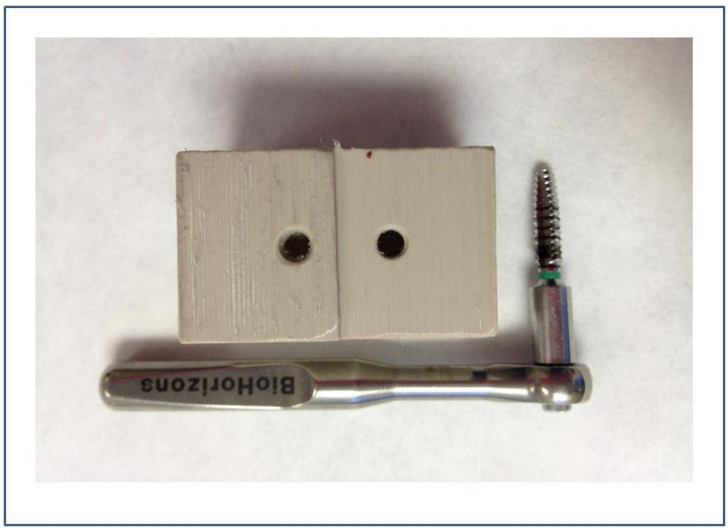

Figure 26. Custom made PEEK torquing device

The custom device with the implant was secured in a clamping device before torquing was performed (Figure 27). When the torquing was completed, the screw access hole was sealed with Teflon tape (Figure 28) and filled with Telio CS Inlay/Onlay (Ivoclar Vivadent Inc. Amherst, NY).

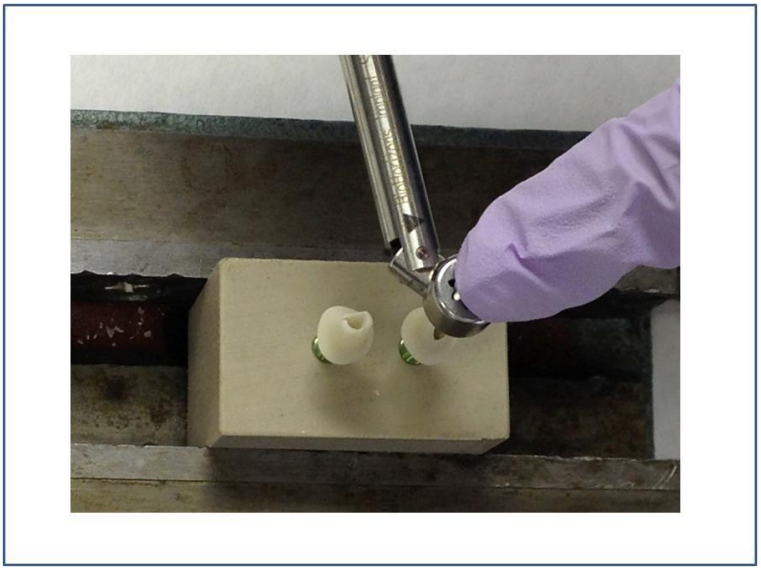

Figure 27. Torquing abutment

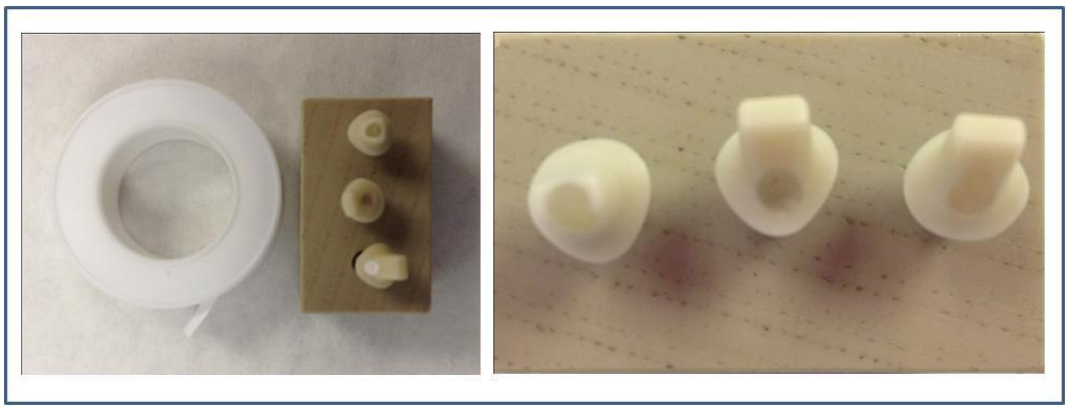

Figure 28. Screw access hole sealed with Teflon tape and Telio CS

3. Cementation of Zirconia Crowns on the Abutment

The zirconia crown was cemented on the abutment under 2Kg of force using resin modified glass ionomer cement (RelyX Luting Plus Luting cement from 3M ESPE, St.Paul, MN). To accomplish this, the implant with the torqued abutment was secured in the previously made PEEK custom device. The PEEK custom device with predrilled implant threads acted as a stable holding base for the implant while the crown is being cemented. The cement was mixed according to the manufacture's instructions and the crown was loaded and seated on the abutment. A 2Kg force was applied to ensure full seating of the crown (Figure 29) and the excess cement was carefully removed. The cement was allowed to set for full 10 minutes.

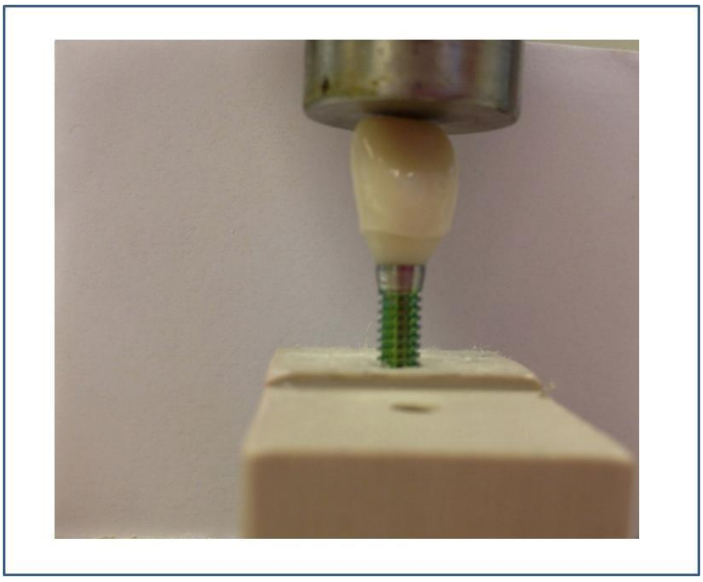

Figure 29. Crown cementation under 2 Kg force

4. Steam Autoclaving and Thermocycling of the Assembled Samples

Steam autoclaving was done to induce phase transformation in zirconia abutment, which is thermally activated and accelerated in presence of water. The implant-abutment-crown assembly was wrapped in moist towel before autoclaving was performed.

The autoclaving was performed in Steris Amsco Century SG-120 Scientific Gravity Sterilizer (STERIS Corporation, Mentor, OH) for continuous 8 hours at chamber temperature of 123.5 degree centigrade and 2.35 bars of pressure.

Once the steam autoclaving was finished, the samples were subjected to thermocycling in the thermocycling unit (Thermo scientific, UAB machine shop) to artificially age the specimen for 10,000 cycles with a bath temperatures of 5 degree C and 50 degree C, with a dwell time of 30 sec and transfer time of 10 sec. To avoid exposure of samples to water in the thermocycling unit the samples were placed in a plastic bag before subjecting them to thermal changes.

5. Mounting the Samples in the Specimen Holder

The samples were mounted in the specimen holder using PMMA (Orthodontic resin, Lang Dental Manufacturing Co Inc., Wheeling, IL) as the mounting medium. The mounting jig previously fabricated was used to consistently mount all the samples. The mounting jig was indexed to align with the mid facial of the zirconia crown (Figure 30). Additionally, all the specimen holders were marked to have one surface identified as facial.

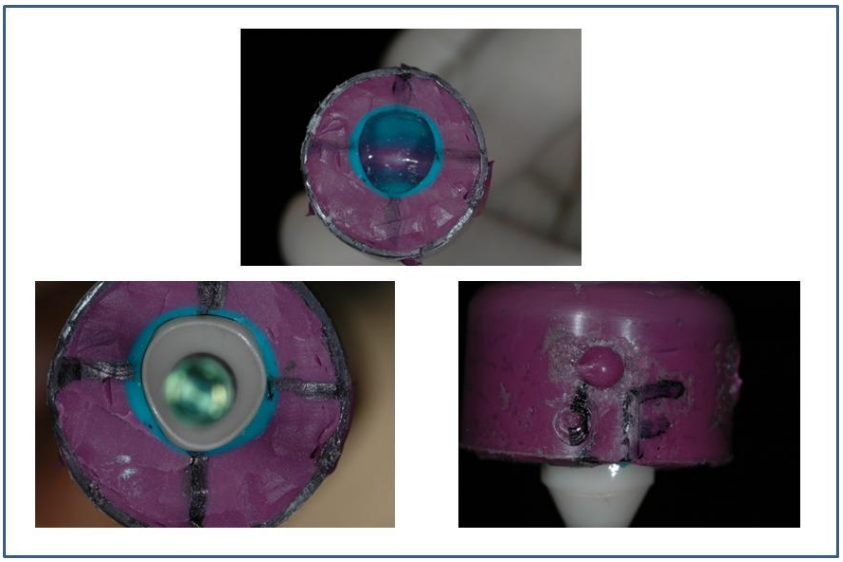

Figure 30. Mounting Jig indexed with respect to the crown

The flat plane on the surveyor table was oriented perpendicular to the analyzing rod with the help of level gauge (Figure 31). The mid point of the square specimen holder was identified and the specimen holder was placed on the flat plane with the midpoint directly under the analyzing rod. At this point, the position of the specimen on the flat plane was marked (Figure 31). This helped position all the specimen holders consistently on the flat plane for successive mounting.

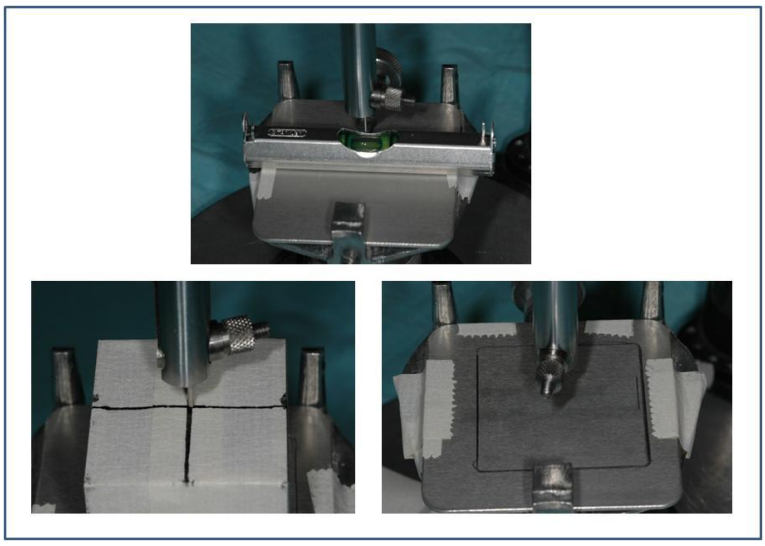

Figure 31. Positioning specimen holder

The crown part of the sample was then fitted on to the mounting jig and the mounting jig with the sample was then attached to the surveyor which will automatically align the implant to its predetermined angulation (Figure 32).

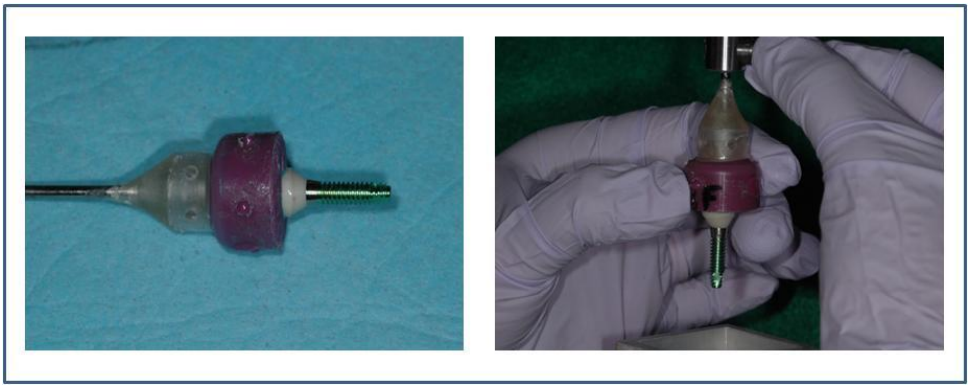

Figure 32. Mounting jig with the assembled sample ready for mounting

The specimen holder was positioned on the previously marked area on the flat plane on the table (Figure 33).

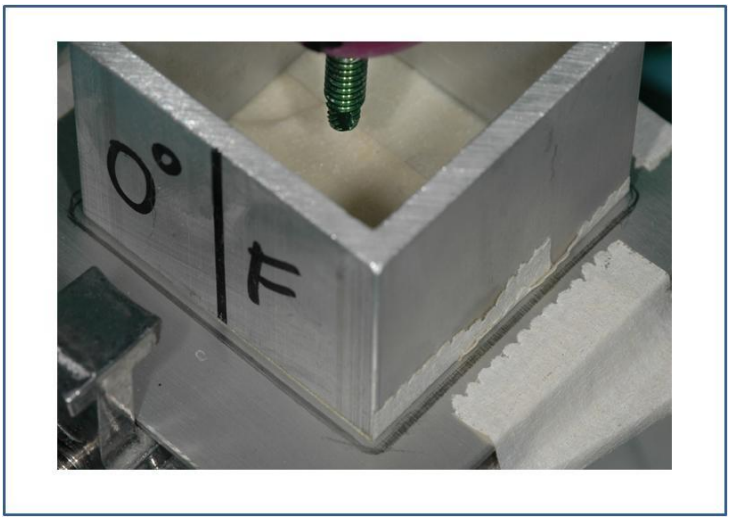

Figure 33. Orientation of the specimen holder

The mounting jig was lowered to the holder at the predetermined depth (Figure 34) so that the implant-abutment interface will be positioned above the surface of the mounting medium. Also it was oriented in such a way so the facial mark on the mounting jig aligned with the facial mark on the specimen holder (Figure 34).

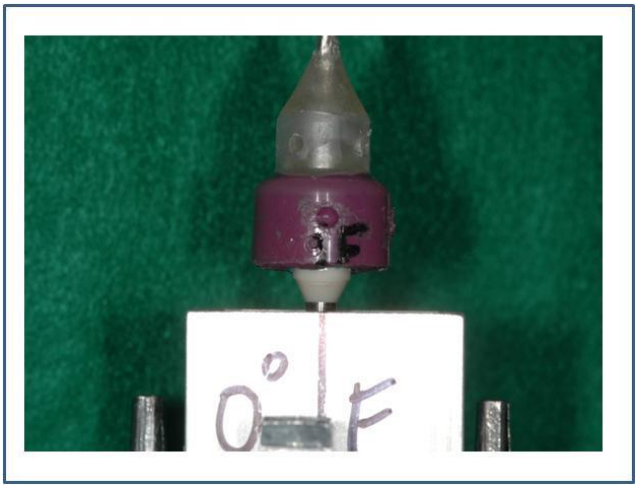

Figure 34. Orientation of mounting jig and specimen holder

The vertical arm of the surveyor was also marked to serve as a reference point for future lowering and accurate positioning of the mounting jig at the predetermined depth. The orientation of the sample from all the three groups inside the specimen holder is shown in Figure 35.

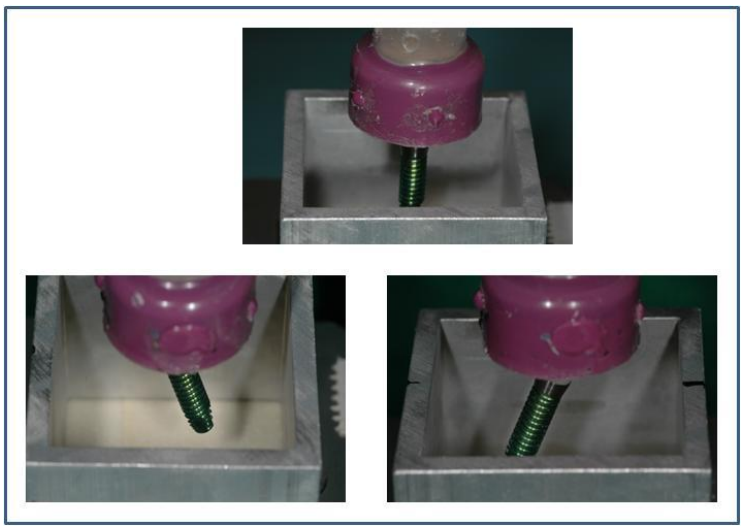

Figure 35. Alignment of the implant to the predetermined angulation

At this point, the PMMA was mixed and poured into the holder (Figure 36) and allowed to set. All the 30 samples were mounted repeating the same technique.

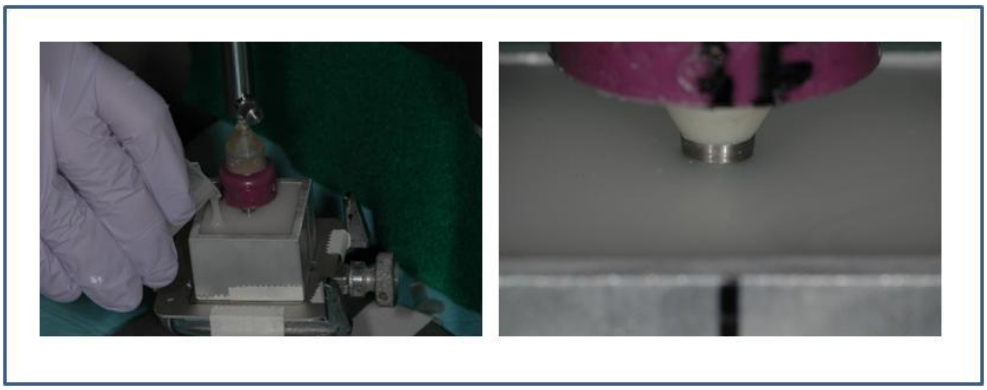

Figure 36. Mounting samples in PMMA

Mechanical Testing

For mechanical testing, the specimens were mounted to provide a 135° relationship between the long axis of the simulated maxillary incisor (supported by the implant) and the mandibular incisor (the indenter) according to the well-established cephalometric interincisal relationships.[39] This was done to closely mimic the off axis loading of the central incisor in the mouth.

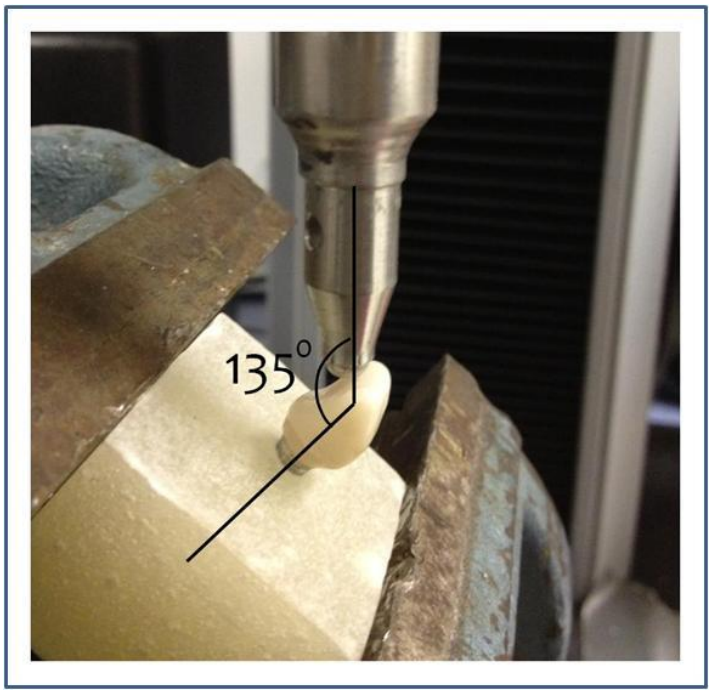

Figure 37. Indenter-crown orientation to simulate the interincisal angle of 135^0

An Instron 811 Universal Testing System (Instron Corporation, Norwood, MA) was used to load the abutments to failure with a cross-head speed of 1 mm/min. A rounded indenter was attached to the cross-head, and the platform with the specimen was oriented in such a way that the long axis of the indenter was aligned at 45 degrees to the long-axis of the mounted zirconia crown on the lingual side (Figure 38).

The indenter was positioned about 2mm from the incisal edge to prevent inadvertent surface damage by the loading stylus on the crown, and a thin layer of mylar film (0.1mm thick) was inserted between the stylus and the crown. Proper safety equipment was worn at all the time to avoid injury from ceramic fracturing.

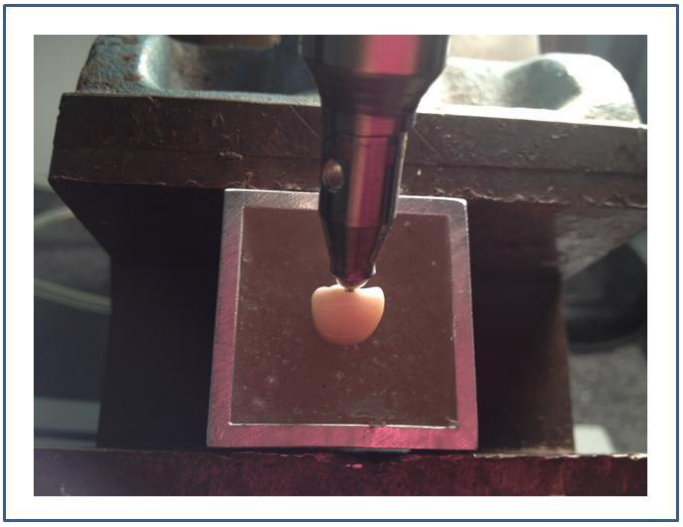

Figure 38. The sample loaded in the Instron machine

Prior to testing, the load cell was calibrated to zero load, and the test commenced by applying a load in displacement control until fracture occurred which was detected by an audible crack and a sudden drop in the force as seen in the graph. Force versus time data was captured via an attached computer. The data was analyzed to determine the load at the fracture.

RESULTS

Fracture Strength

A plot of the applied force versus distance as recorded by the Instron machine was generated for all experimental runs. A typical loading curve is illustrated below (Figure 39) and the fracture of the abutment is indicated by a sudden drop in the force value.

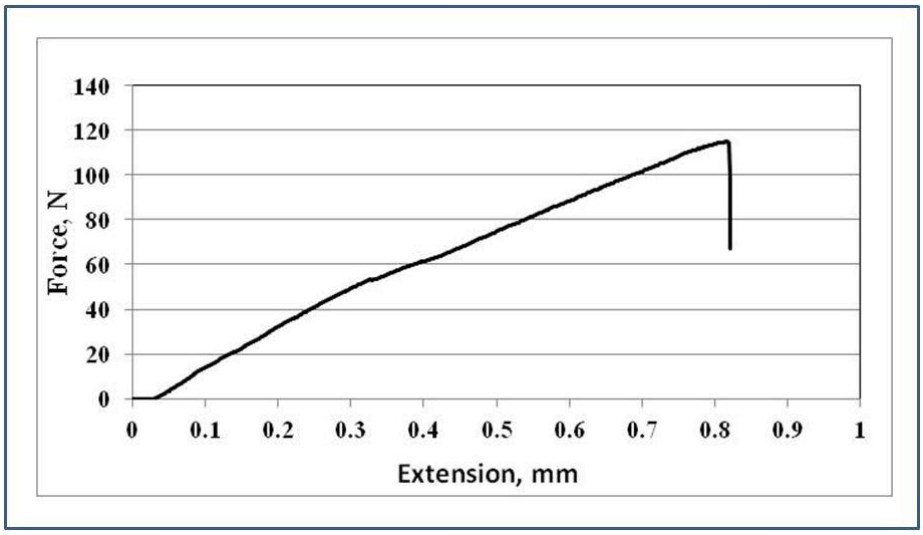

Figure 39. Loading curve for 0 degree untreated (group 1 - sample #5)

In group 1, sample 3 and sample 7 did not produce the typical loading curve, the force value increased at a steady rate for a particular distance and then accelerated. At this point the testing was stopped, the sample was retrieved and examined. It was found that the abutment was broken. Hence the load at fracture was determined to be the point where a change in the slope of the curve is detected (Figure 40).

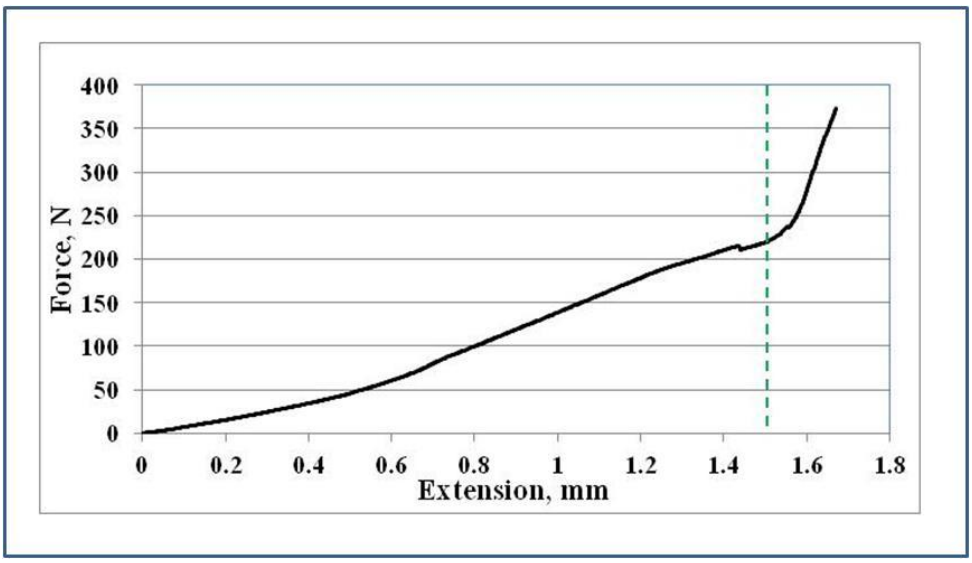

Figure 40. Loading curve for 0 degree untreated (group 1 - sample #3)

In group 2, all samples produced the typical loading curve. The curve for sample 2 in group 2 is shown in Figure 41.

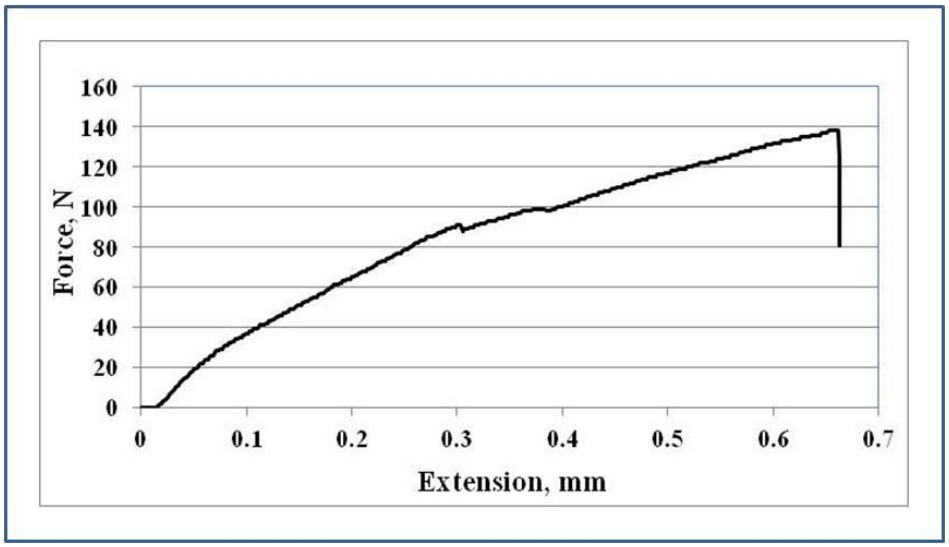

Figure 41. Loading curve for 20B untreated (group 2 - sample #2)

In group 3, all samples produced the typical loading curve. The curve for sample 3 in group 3 is shown in Figure 42.

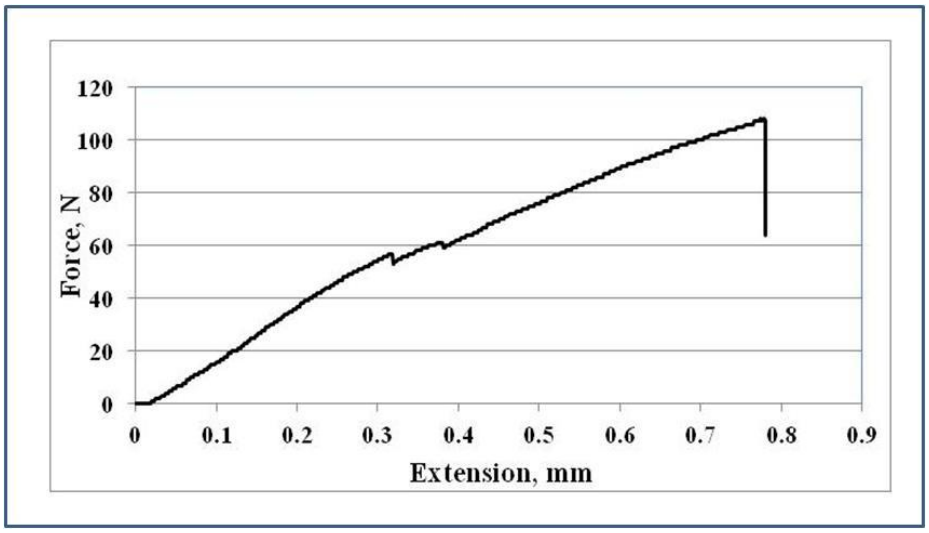

Figure 42. Loading curve for 20L untreated (group 3 - sample #3)

In group 4, all samples except sample #3 produced the typical loading curve. The curve for sample 3 is shown in Figure 43 and the curve for sample 6 in Figure 44.

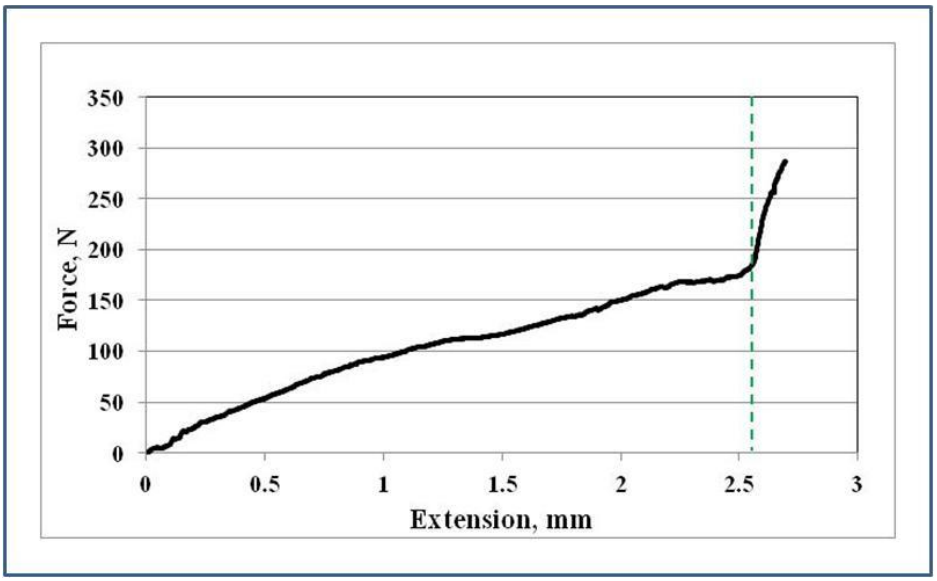

Figure 43. Loading curve for 0 degree treated (group 4 - sample #3)

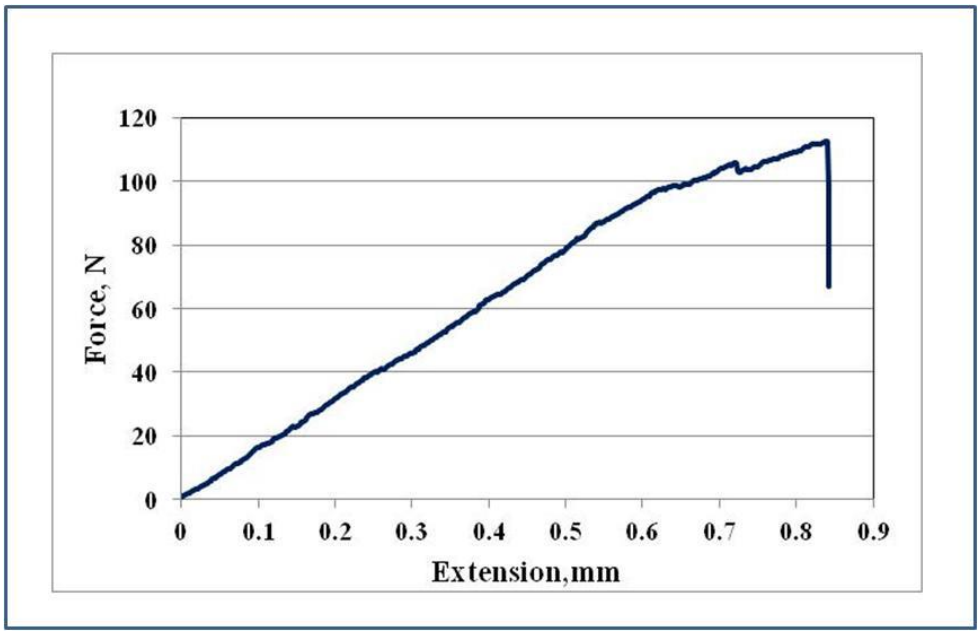

Figure 44. Loading curve for 0 degree treated (group 4 - sample #6)

In group 5, all samples except sample #4 and #6 produced a typical loading curve. The curve for sample 4 is shown in Figure 45 and the curve for sample 8 in Figure 46.

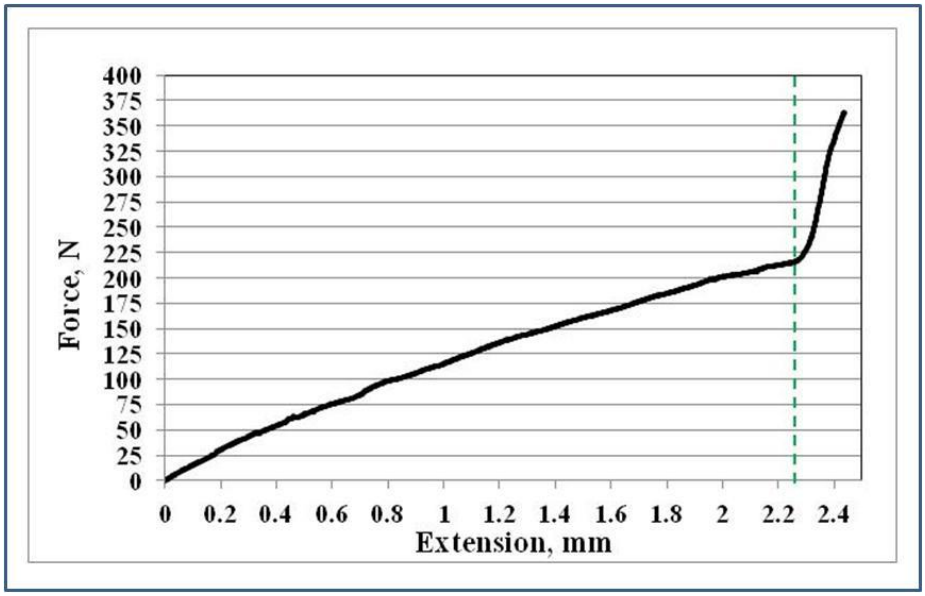

Figure 45. Loading curve for 20B treated (group 5 - sample #4)

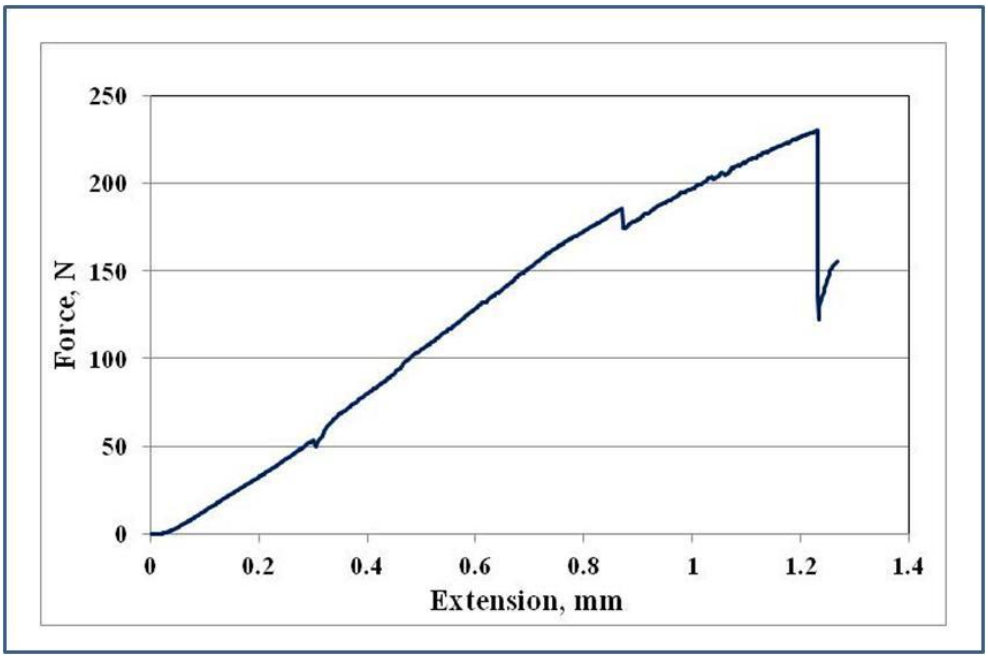

Figure 46. Loading curve for 20B treated (group 5 - sample #8)

In group 6, all samples produced the typical loading curve. The curve for a sample 6 in group 6 is shown in Figure 47.

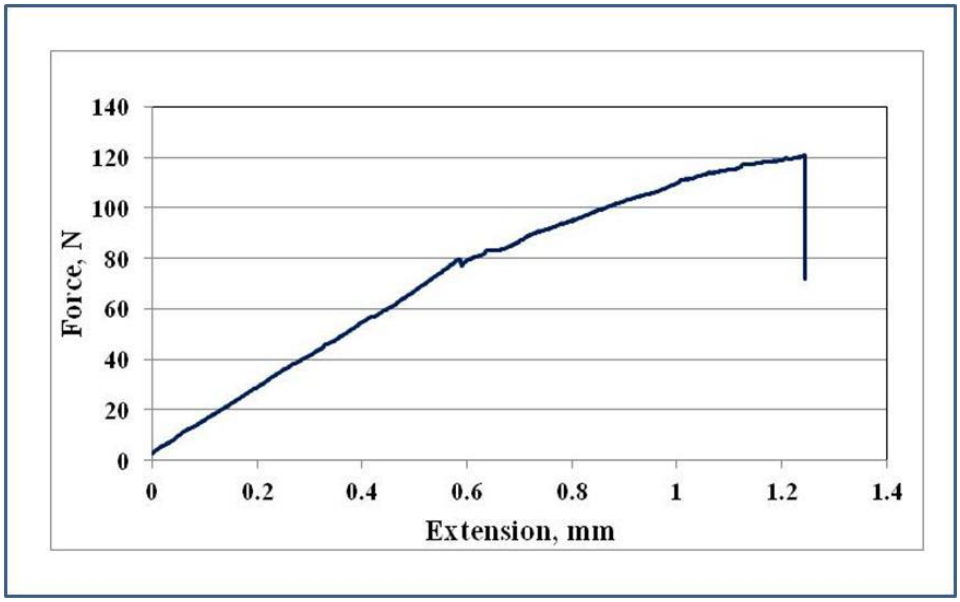

Figure 47. Loading curve for 20L treated (group 6 - sample #6)

The force value (N) at abutment fracture determined from the analysis of the curves for all samples is listed in Table.2 and represented in Figure 48 and 49. In all the experiments, the abutment broke at various points whereas the crowns did not fracture, crack or chip. Moreover, the PMMA assembly did not crack or chip. The implant platform appeared intact. Hence the force at failure determined in these experiments represents the force value to break the abutment.

Table.2. Summary of load to facture experimental results

Sample number	0 degree group 1	20 F group 2	20 L group 3	0 degree group 4	20 F group 5	20 L group 6
1	130.25	143.41	123.59	103.56	243.30	130.96
2	203.90	138.25	114.27	134.15	208.81	94.03
3	214.22	129.40	107.69	176.21	290.29	114.06
4	96.93	117.93	110.75	107.76	216.44	110.39
5	114.99	107.96	108.59	107.89		122.89
6	97.47	116.28	117.76	112.52	216.44	120.89
7	164.88	126.84	162.03	120.32	233.44	129.30
8	107.36	115.05	119.35	96.42	230.15	129.92
9	159.67	119.72	111.55	129.72	239.19	105.08
10		153.16	125.90	93.45	255.05	108.14
Mean	143.30	126.80	120.15	118.20	237.01	116.57
SD	44.65	14.30	15.95	24.28	24.77	12.30

In group 1, sample 10 was loaded incorrectly and the experiment did not go to completion. In group 5, the sample was aligned incorrectly. Even though testing was completed, the fracture value was much less than the other samples in the groups. Hence these samples were discarded from the analysis.

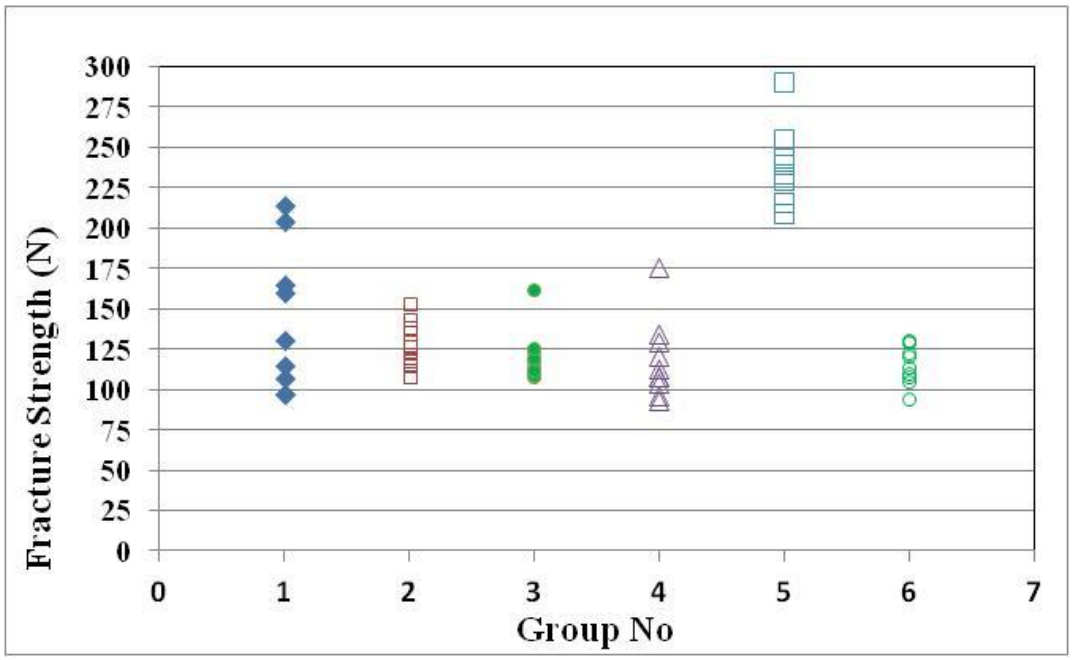

Figure 48. Scatter plot of the load to fracture

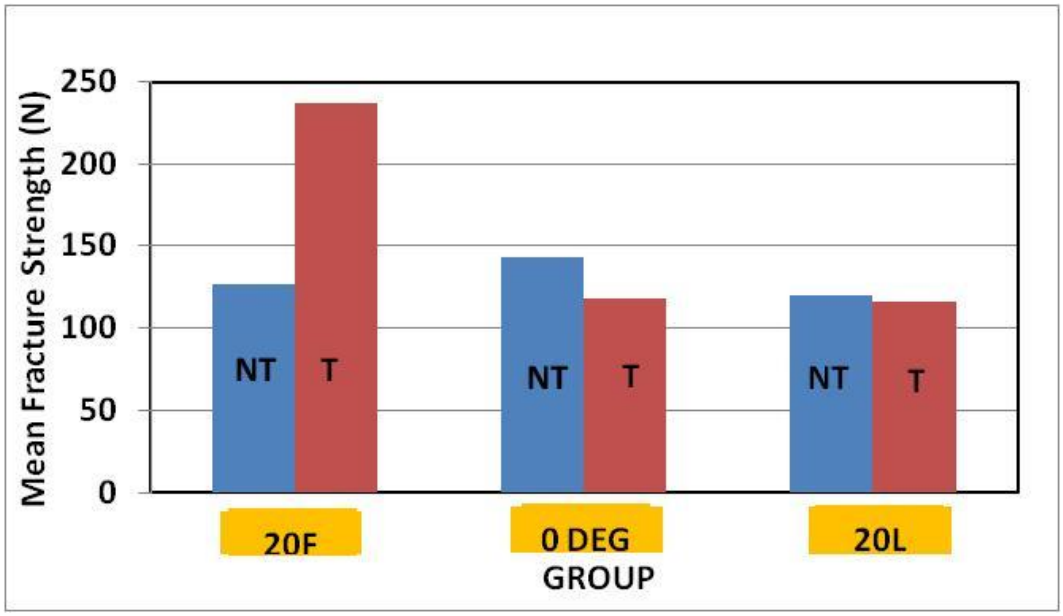

Figure 49. Results summary
(NT-Not Treated, T-Treated, steam autoclaving and thermocycling)

Statistics

The data for all the groups were analyzed using two-way ANOVA. A non-parametric two factor ANOVA based on rankings was completed since the data is found to be not normally distributed. This analysis showed that effect of implant angle on the fracture strength is statistically significant ($F(2,52) = 12.25$ $p < 0.001$).

F Test for RankMPa					
Grouping Variable: Angle					
Hypothesized Ratio = 1					
	Var. Ratio	Num. DF	Den. DF	F-Value	P-Value
0, F	1.646	18	18	1.646	0.2997
0, L	2.486	18	19	2.486	0.0574
F, L	1.511	18	19	1.511	0.3832

ANOVA Table for RankMPa							
	DF	Sum of Sq	Mean Squa	F-Value	P-Value	Lambda	Power
Treatment	1	286.667	286.667	1.633	0.207	1.633	0.227
Angle	2	4301.663	2150.831	12.251	<.0001	24.502	0.997
Treatment * Angle	2	2777.979	1388.989	7.912	0.001	15.823	0.955
Residual	52	9129.389	175.565				

Comparison between groups (Tukeys HSD) showed that whereas the variation between 0 degree and 20F, between 20F and 20 L are statistically significant, the variation between 0 degree and 20L is not statistically significant. Hence it is concluded that fracture strength of zirconia abutment is influenced by the varying implant angulation and hypothesis 1 is rejected.

Tukey/Kramer for RankMPa			
Effect: Angle			
Significance Level: 5 %			
	Mean Diff.	Crit. Diff	
0, F	-17.053	10.384	**S**
0, L	1.471	10.253	
F, L	18.524	10.253	**S**

Similarly, the effect of treatment (thermal degradation and thermocycling) is evaluated using two-way ANOVA. A non-parametric two factor ANOVA based on rankings was completed since the data is found to be not normally distributed. The result showed that treatment alone has no effect on the fracture strength ($F(2,52)=1.633$, p value=0.207). The higher fracture strength exhibited by 20F in group 5 is contingent upon treatment as demonstrated by the significant first-order interaction term between treatment and angulation($F(2,52)=7.91$, p value<0.001). Hence it is concluded that while treatment did not influence fracture strength of zirconia abutment overall, under certain circumstances of angulation, thermal degradation and thermal cycling may affect fracture strength.

Tukey/Kramer for RankMPa		
Effect: Treatment		
Significance Level: 5 %		
	Mean Diff.	Crit. Diff
t1, t2	-3.759	6.993

Interaction Line Plot for RankMPa					
Effect: Angle * Treatment					
F Test for RankMPa					
Grouping Variable: Treatment					
Hypothesized Ratio = 1					
	Var. Ratio	Num. DF	Den. DF	F-Value	P-Value
t1, t2	0.497	28	28	0.497	0.0691

Fracture Analysis

Fractured samples were carefully collected and labeled for fracture analysis. Individual samples from every group are imaged under Keyance microscope (VHX-600 series) at 40 times magnification.

Three types of breakage were observed in the untreated and treated groups.

Pattern A: two level fracture - abutment fracture at the hex portion and slightly above the platform.

Pattern B: one level fracture - abutment fracture at the hex portion only.

Pattern C: one level fracture - abutment fracture slightly above the implant platform.

These patterns are demonstrated in Figures 50 to 54. In majority of the samples (93.2%), patter A fracture was observed. The pattern B fracture was observed in 3 samples (5.1%) and pattern C fracture was observed in 1 sample (1.7%). In the samples where the abutment fractured slightly above the implant platform, observation under light microscopy at 40 times magnification revealed that the fracture was single planar on the lingual side (Figure 55) and multiplanar on the facial side (Figure 56). This pattern is suggestive of the fact that fracture started on the lingual, which is the side subjected to tension. The overlaying crown, implant or PMMA did not break in any of the samples during the loading.

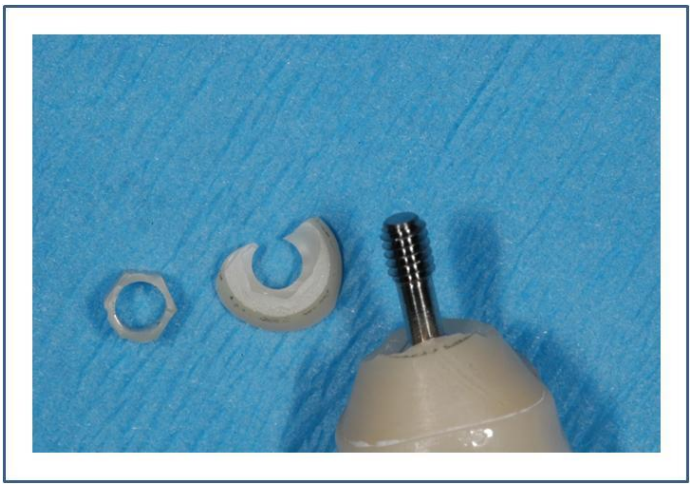

Figure 50. Pattern A fracture; both hex portion and area slightly above the platform broke (group 1 - sample #1)

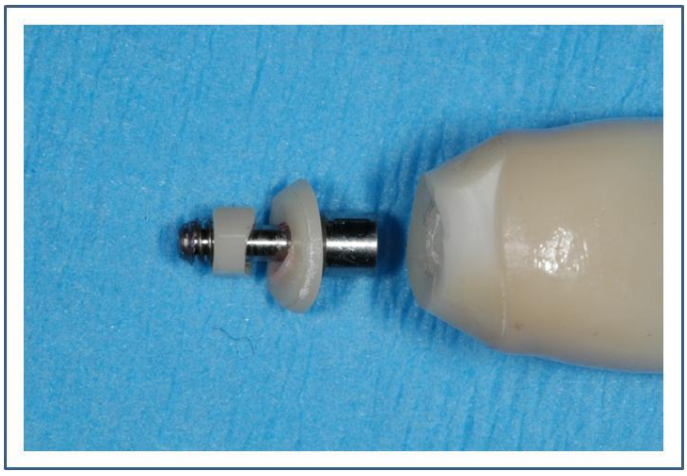

Figure 51. Pattern A fracture; both hex portion and area slightly above the platform broke (group 1 - sample #9)

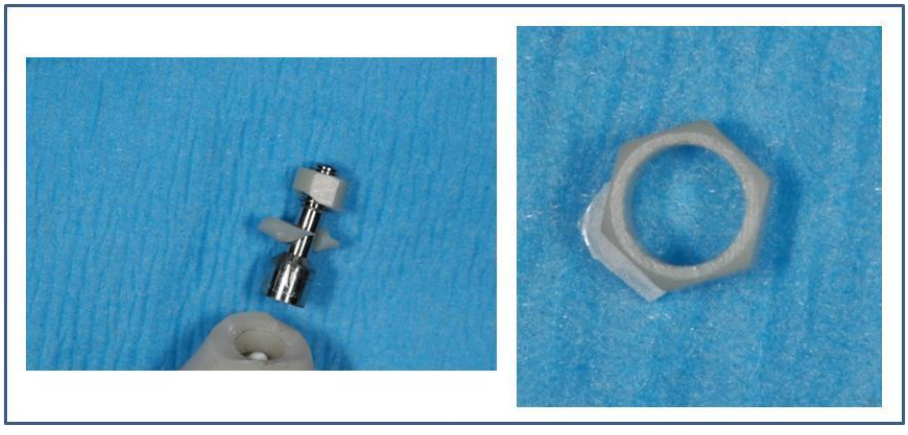

Figure 52. Pattern A fracture; both hex portion and area slightly above the platform broke (group 2 - sample #1)

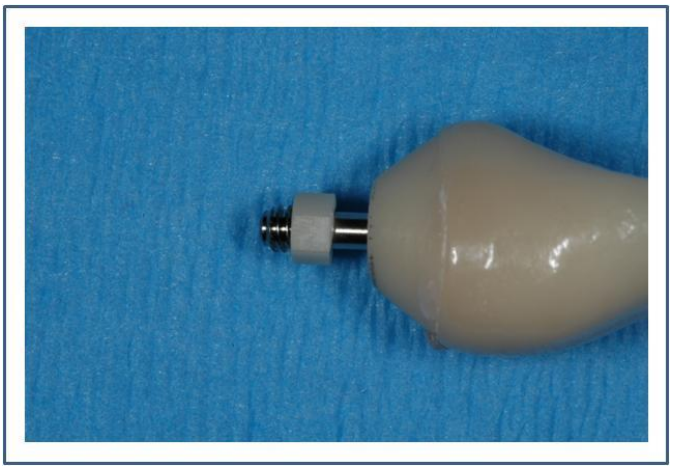

Figure 53. Pattern B fracture; only hex portion broke off (group 1 - sample #7)

Figure 54. Pattern C fracture; abutment fracture slightly above the implant platform and the hex portion survived (group 4 - sample #1)

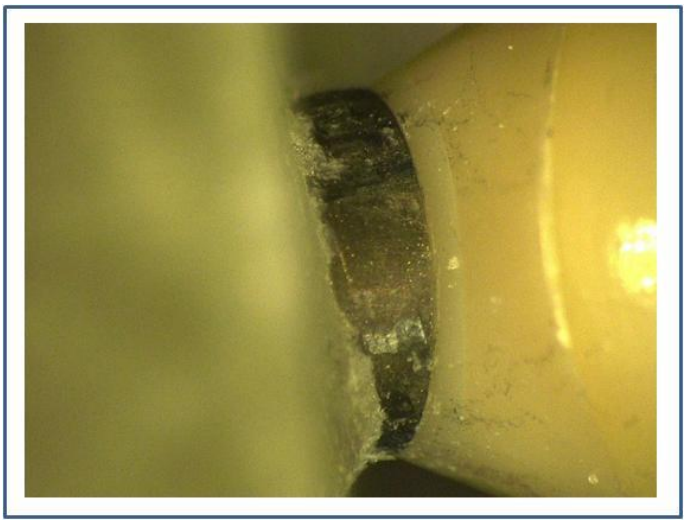

Figure 55. Typical fracture pattern on the lingual side (group 3 sample #2)

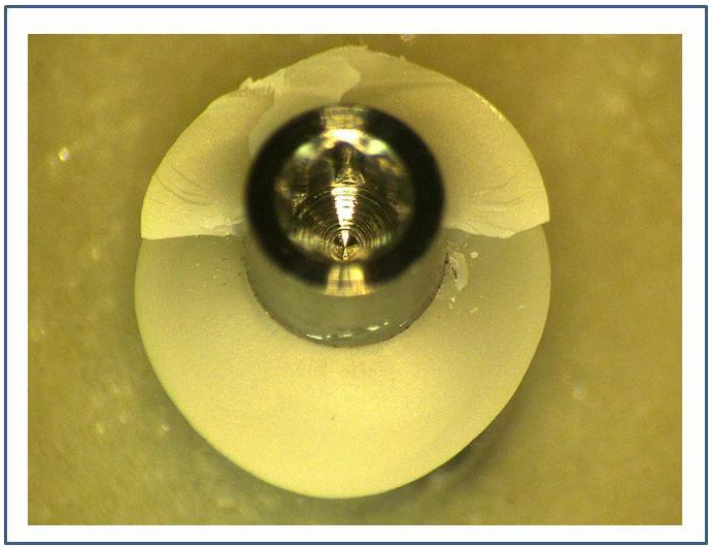

Figure 56. Multiple layer fracture on the facial side and single plane fracture on the lingual side (group 3 sample #8)

Table.3. Summary of fracture mode - untreated groups

Sample number	0 degree group 1	20 F group 2	20 L group 3
1	hex portion & slightly above platform	hex portion & slightly above platform	hex portion & slightly above platform
2	**hex portion only**	hex portion & slightly above platform	hex portion & slightly above platform
3	hex portion & slightly above platform	hex portion & slightly above platform	hex portion & slightly above platform
4	hex portion & slightly above platform	hex portion & slightly above platform	hex portion & slightly above platform
5	hex portion & slightly above platform	hex portion & slightly above platform	hex portion & slightly above platform
6	hex portion & slightly above platform	hex portion & slightly above platform	hex portion & slightly above platform
7	**hex portion only**	hex portion & slightly above platform	hex portion & slightly above platform
8	**hex portion only**	hex portion & slightly above platform	hex portion & slightly above platform
9	hex portion & slightly above platform	hex portion & slightly above platform	hex portion & slightly above platform
10		hex portion & slightly above platform	hex portion & slightly above platform

Table.4. Summary of facture mode - treated groups

Sample number	0 degree group 4	20 F group 5	20 L group 6
1	**slightly above platform only**	hex portion & slightly above platform	hex portion & slightly above platform
2	hex portion & slightly above platform	hex portion & slightly above platform	hex portion & slightly above platform
3	hex portion & slightly above platform	hex portion & slightly above platform	hex portion & slightly above platform
4	hex portion & slightly above platform	hex portion & slightly above platform	hex portion & slightly above platform
5	hex portion & slightly above platform	hex portion & slightly above platform	hex portion & slightly above platform
6	hex portion & slightly above platform	hex portion & slightly above platform	hex portion & slightly above platform
7	hex portion & slightly above platform	hex portion & slightly above platform	hex portion & slightly above platform
8	hex portion & slightly above platform	hex portion & slightly above platform	hex portion & slightly above platform
9	hex portion & slightly above platform	hex portion & slightly above platform	hex portion & slightly above platform
10	hex portion & slightly above platform	hex portion & slightly above platform	hex portion & slightly above platform

DISCUSSION

Angulation And Fracture Strength

The primary purpose of this study was to evaluate the correlation between the fracture strength of customized zirconia abutment and varied abutment designs produced by the modifying implant angulations namely the 0 degree, 20F and 20L. Since the samples in this study consisted of an implant-abutment-crown assembly, care has been taken in the design of the samples to keep the abutment design as the only variable. This eliminated all the other variables that could potentially arise from varied crown design or varied implant design. Thus the crowns were standardized in terms of material and dimensions. The CAD-CAM technology was utilized to generate monolithic zirconia crown which were identical both in external and internal dimensions, marginal contours etc., so that it can precisely fit all the abutments in an identical fashion. A monolithic crown was selected to eliminate the possibility of the crown becoming the weak link thus avoiding a potential crown fracture during the loading process. The angle corrected customized abutments from every group differ primarily in terms of emergence profile and screw hole location but are uniquely similar in terms of marginal contours and dimensions so that it can fit all the crowns precisely.

1. Screw Hole Location And Fracture Strength

The difference in the screw hole location affected the facial and lingual dimensions of the abutment (Figure 13). The facial and lingual dimension of the abutments were recorded and found to be different in every group. The lingual dimensions are critical and should be looked into carefully as the lingual side is the area subjected to tension and facial side is subjected to compression during occlusal loading. The dimensions on the lingual side (the thickness from the screw hole to the outside surface) were the highest for the 20L group followed by 0 degree group and least for the 20F group (20F 1.46 mm, 0 degree 2.53 mm, 20L 2.71 mm).

The hypothesis of this study was that varied screw hole location and varied lingual dimension have a tremendous effect on the fracture strength of the customized abutment. Statistical analysis of study results showed that fracture strength was highest for the 20F and lowest for the 20L. Thus the fracture strength and the thickness at the lingual aspect have an inverse relationship to each other. This observation reveals that variation in lingual dimensions because of the varied screw hole location is not a controlling factor in the fracture strength of the abutment. This could possibly be due to the stress shielding effect of the monolithic zirconia crown covering the abutment from the effects of occlusal forces during the loading. The results of this study showed that none of the crowns fractured during the loading process. Studies that tested the fracture strength of the zirconia abutment without the full veneer crown is not a true clinical representation and it may not reflect the accurate fracture strength in vivo. This study was designed to closely simulate in vivo conditions by utilizing the zirconia abutment and zirconia crown, which is the current state of art in implant prosthodontics.

2. Emergence Profile And Fracture Strength

The effect of varied emergence profile of the abutment on the fracture strength was also examined in this study. To accommodate the variation in the implant angulation and to keep the gingival contour of the abutment as a constant factor for all the groups was a challenging task, but was accomplished in this study. This design produced abutments with varied emergence profile that had different occluso-gingival height in the facial and lingual aspects (Figures 12). The group 2 and 5 where the implant is angulated to the facial had the longest occluso-gingival dimension on the lingual side. The group 3 and 6 where the implant is angulated to the lingual had the shortest occluso-gingival dimension on the lingual side.

As mentioned before, the abutment dimension on the lingual side is critical as the lingual aspect is subjected to tension during the occlusal loading. The results of this study showed that the occluso-gingival dimension of the abutment on the lingual side might have contributed to the facture strength of the abutment. It was found that the fracture strength values were directly proportional to the abutment dimension in the occluso-gingival aspect from the implant platform to the gingival margin. The occluso-gingival dimension of the abutment on the lingual side was highest for the 20F group followed by 0 degree group and least for the 20L group (20F=3.17 mm, 0 degree=2.52 mm, 20L=2.09 mm).

This correlation is reflected in the statistical analysis of this study result which concludes that angulation has a statistically significant influence on the fracture strength of the abutment. None of the previous studies examined these factors in detail.

Angulation And The Resultant Force Vectors

The varied angulation of the implants with the uniquely differing abutments presented a complex geometry of implant-abutment-crown assembly. It is important to observe if there is any correlation between a particular geometry and its ability to withstand relatively higher occlussal forces. The picture below is diagrammatic representation of variation of resultant force vectors on a particular geometry. In this diagram one can see that for the same amount of applied force (100 N), the resultant vector force that can produce tensile stress on the lingual side can be quite different from one group to another. Quantitative biomechanical analysis of the resultant forces (Figure 57) revealed that when the implant apex gets tilted towards the facial as in 20 degree facial group, it can survive more occlussal force before it fractures compared to 0 degree and 20 degree L. This is reflected in the results from this study that clearly showed that force values for the 20F group is highest followed by 0 degree and the lowest for the 20L. Thus this study results support the importance of grafting prior to implant placement to avoid lingual placement of implant. Angulation of the implant apex towards the lingual usually happens in scenarios where there is resorption of the facial cortical plate or from surgical errors in implant placement from not utilizing a surgical guide.

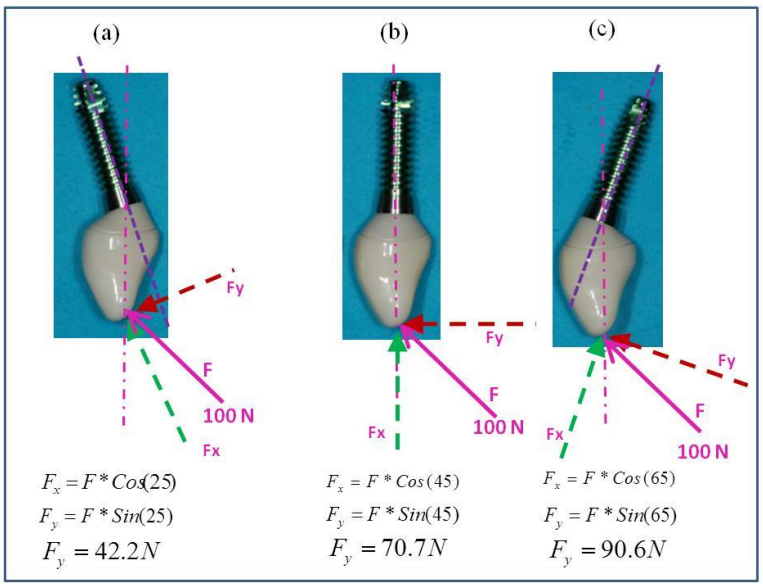

Figure 57. Influence of angulation on the resultant force vectors

(a) 20 degree facial (b) 0 degree (c) 20 degree lingual

Angulation And Fracture Mode

The results of this study could not find a correlation between the fracture mode in the abutments and the varied angulations as comparable fracture pattern was observed in all the abutments from the three different angulation groups. In general fracture of the zirconia abutment occurred at the cervical portion of the abutment, near the screw and platform of the implant. This area has been presumed to be an area of the highest torque and stress concentrations due to the levering effect.[17-22] In majority of the samples, the hex portion of the abutment broke off (Table 3, Table 4). This finding suggested that hex was the weak link in the entire abutment and it might have broken first. The dimension of the hex portion of the abutment was 0.14 mm and at the implant platform was 1.25 mm (Figures 58).

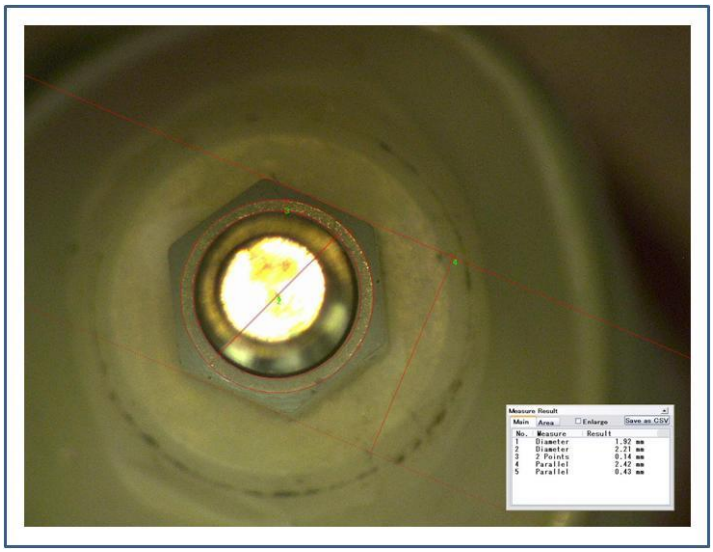

Figure 58. Measurement of the hex portion of the abutment

Previous studies that correlated the thickness of zirconia to the fracture strength reported that fracture strength drops significantly when the thickness is reduced beyond 0.5 mm - 0.7 mm. [24.] So the inadequate thickness of the hex portion at the implant-abutment interface could be the reason for the consistent nature of the fracture at this location. The importance of using a secondary metallic component to reinforce the zirconia abutment at the implant-abutment interface has been discussed in a previous study by Sailer et. al.[26] The same study found that when the secondary metallic insert has not been used, the reason for failure was abutment fracture. In samples where metallic inserts were used with the zirconia abutments, plastic deformation of the metallic components was found in addition to or prior to abutment fracture. Also the results of the same study concluded that two piece zirconia abutments with a secondary coupling abutment or a metallic insert exhibited significantly higher bending moments than one piece internally or externally connected abutments.

In the samples where the abutment fractured slightly above the implant platform, observation under light microscopy at 40 times magnification revealed that the fracture is single planar on the lingual side (Figure 55) and multiplanar on the facial side (Figure 56). This pattern is suggestive of the fact that fracture started on the lingual, which is the side subjected to tension. Thus the increased occluso-gingival height at the lingual side of samples in the 20F group might have contributed to the highest fracture strength in that group.

Implant Abutment Connection And Fracture Resistance

It is interesting to note that fracture resistance of zirconia abutments is lower than the force values (184N- 793N) obtained in comparable previous studies.[17,18,20,21,22] In general the force values reported varied dramatically from one study to another due to variations in the study designs. Implant-abutment connection could be a controlling factor when it comes to the location of fracture, the mode of the fracture and the possible fracture resistance of a particular abutment. Previous study by Sailer et. al.[26] concluded that the type of connection significantly influenced the strength of zirconia abutments. Essentially the implant's internal or external connection geometry controls the abutment design in terms of morphology and dimensions. Thus the configuration of an abutment that is deigned to fit a shorter internal hex is quite different than one that is designed to fit an implant with a conical internal connection or an external connection. For example, in a previous study by Adita et.al[20] where they tested the fracture strength of zirconia abutment with a conical connection, the force values and the fracture mode were different. The fracture location seemed to be comparable to this study where the fracture occurred at the thinnest portion of the abutment at the abutment-implant interface and

localized to one site. In this study an internal shorter hex implant was used, not only did the hex portion break off but the portion slightly above the implant platform also broke off in majority of the samples. This could be attributed to the geometrical differences between the abutment designs due to the implant-abutment connection differences. It is important to note that the same study did not use a full crown on the abutment but the force values were higher than the force values obtained in this study. Again this could be because of the difference in stress transfer mechanism from the abutment on to the implant from one connection design to the other.

Merz et.al[28] elaborated on the merits of conical connections and suggested that in conical connection, lateral loading is resisted mainly by the taper interface, which prevents the abutment from titling off, even when the connection between the taper section and the hex of the abutment is lost, for example because of a fracture. In another comparable study[22] where they examined the fracture resistance of zirconia abutment using abutments with conical connection, the force values for the straight and the angulated abutment came out higher than the force value in this study which again leads to the speculation that the abutment with long conical connections may outperform abutments with short hexagonal connection in terms of fracture strength. The fracture location in the above mentioned study was much below the implant platform in the region of the internal hexagon where the abutment is thinnest. This is different from the fracture location in this study, which was either at the hex or both at the hex portion and slightly above the platform. Thus the commonality of this study and the previous studies is that in all the studies the fracture location is always at the weak portion of the abutment where it is the thinnest, but the location and the fracture strength varied from one study to another.

This could be from the varied abutment connection geometry from one study to another. This is the first study that evaluated the fracture strength of zirconia abutment when used in conjunction with an implant with shorter internal connection.

Aging And Fracture Strength

Steam autoclaving and thermocycling has been done to simulate the effects of aging in vivo and the results showed that aging did not have a statistically significant influence on the fracture strength of abutments. Low temperature degradation is a highly complex and multifactorial process. It has been proved[40] that low temperature aging produced both positive and negative effects on the mechanical properties of Y-TZP ceramics depending on the temperature applied.[39] The same study concluded that when aging at temperature below 125°C for 10 hours was applied, the flexural strength of Y-TZP ceramics increased. However, aging above 150°C, the flexural strength started to decrease. In this study, it was speculated that the reason for a slight increase in fracture strength of the treated 20F group could be attributed to the strengthening effect of LTD because the aging temperature and time that were chosen for this study were 123 and 8 hrs respectively and this satisfies the time and temperature requirement for an improved fracture strength.[39] But in this study a similar correlation between the treated and untreated group in the 20L and 0 degree category could not be found. So it can be concluded that while treatment did not influence the fracture strength of zirconia abutment overall, under certain circumstances of angulation thermal degradation and thermocycling may have an effect in fracture strength. This needs further investigation.

A recently published study[41] that examined the effect of LTD (100 degree Celsius for 7 days) on the flexural strength of zirconia reported that LTD did not affect the

flexural strength of Y-TZP. Alghazzawi et.al[41] used relatively much higher time compared to what was used in this study, which is only 8 hrs. The same study also reported that the tetragonal to monoclinic transformation occurred in the external surface only with shallower depth, and the internal flaws were not critical enough to affect the flexural strength. Our study results has substantiated the results from Alghazzawi et.al[41] study since the fracture resistance of treated and untreated groups did not show any difference in the 20L and the 0 degree group.

Anterior Bite Force And Fracture Strength

Force values measured in the anterior region ranged from 90N -370N.[42] The mean fracture strength of abutment in 20F was 179.01 N, for 0 degree was 130.1 N, and for 20Lwas 118.36 N. This is much lower than what has been observed in the previous studies and may not be sufficient to withstand the occlussal forces in the anterior region in all the treatment population. This could be attributed to the particular geometry of the abutment that is designed to fit the implant used in this study. In general, data on the fracture strength of zirconia abutments are difficult to compare between studies because of the difference in the study design. The implant chosen for this study had a tapered internal hex of 1.5mm. It was also found in this study that hex portion of the abutment measured only 0.14 mm which is much thinner than the minimum required thickness[24] (0.5mm -0.7 mm) for resisting the bending forces. It was postulated that incorporating a metallic insert into the one piece abutment would improve the fracture strength and is beneficial when using implants with shorter internal connection. This area needs further investigation. The force values that could be obtained with the use of a different implant system with deeper internal connection also need further investigation.

Clinical Significance

This study has been designed to closely simulate the in vivo conditions. The test model has been carefully designed with zirconia crown and zirconia abutment which is the current state of art in implant prosthodontics. The loading angle, loading point, aging treatments and surgical errors have also been simulated to represent the intra oral conditions. After analyzing the results from this study, zirconia with secondary metallic insert or anodized titanium abutment is recommended when the implant abutment connection is shorter and when the internal connection area of the zirconia abutment lacks the minimum thickness recommended (0.5-0.7mm) for fracture resistance. Increasing the distance from the platform to the gingival margin on the lingual side of the abutment may be beneficial to improve the fracture resistance of the zirconia abutment. In the anterior zone, where off axial loading is unavoidable, implants with deeper connection may be beneficial when considering zirconia abutments. Grafting is highly recommended when there is resorption of the facial bone to avoid tilting the implant apex in the lingual direction. Finally, utilization of a surgical guide is suggested to avoid surgical errors in placement.

CONCLUSIONS

Within the limitation of this study, it can be concluded that

1) Variation in implant angulation affected the fracture strength of the zirconia abutment. The 20F had the highest fracture strength followed by 0 degree, the 20L had the lowest fracture strength.
2) For the time and temperature used in this study, aging did not seem to affect the fracture strength of zirconia abutment.
3) From the biomechanical stand point, 20F group can sustain more occlussal force than 0 degree and 20L groups.

Recommendations for Future Study

The influence of implant angulations on fracture strength of zirconia abutments with implants with deeper connection needs further investigation. Also it is suggested to investigate the variation in fracture strength of zirconia abutments when the abutments are coupled with metallic inserts. Furthermore, a detailed study of abutment fracture pattern could be beneficial to improve the abutment design.

LIST OF REFERENCES

1. Carl E. Misch. Contemporary Implant Dentistry (Second Edition). St. Louis. Missouri: Mosby Publication, 1999.

2. Noack N, Willer J, Hoffman J. Long-Term Results after Placement of Dental Implants: Longitudinal Study of 1,964 Implants over 16 Years. The International Journal of Oral & Maxillofacial Implants 1999;14:748–755.

3. Ming-Lun Hsu, Fang-Ching Chen, Hung-Chan Kao, Cheng-Kung Cheng. Influence of Off-Axis Loading of an Anterior Maxillary Implant: A 3-dimensional Finite Element Analysis. The International Journal of Oral & Maxillofacial Implants 2007; 22(2):301-309.

4. Rosenberg ES, Torosian JP, Slots J. Microbial differences in 2 clinically distinct types of failures of osseointegrated implants. Clin Oral Implants Res 1991; 2(3):135-144.

5. Sahin S, Cehreli MC, Yalcin E. The influence of functional forces in the biomechanics of implant-supported prosthesis-A review. J Dent 2002; 30:271-282.

6. Tonetti MS. Determination of the success and failure of root form osseointegrated dental implants. Adv Dent Res 1999; 13:173-180.

7. Bidez MW, Misch CE. Force transfer in implant dentistry: Basic concepts and principles. J Oral Implantol 1992:264-274.

8. Brånemark P-I, Zarb GA, Albrektsson T(eds). Tissue-Integrated Prostheses: Osseointegration in Clinical Dentistry. Chicago: Quintessence, 1985:129.

9. Barbier L, Schepers E. Adaptive bone remodeling around oral implants under axial and nonaxial loading conditions in the dog mandible. JOMI 1997; 12(2): 215-223.

10. Sullivan D. Prosthetic considerations for the utilization of osseointegrated fixtures in the partially edentulous arch. Int J Oral Maxillofac Implants 1986; 1:39–45.

11. Weinberg LA. Therapeutic biomechanics concepts and clinical procedures to reduce implant loading. Part I. J Oral Implantol 2001: 27:293-301.

12. Chun-Li Lin, Jen-Chyan Wang, Lance C. Ramp, Peng-Ru Liu. Biomechanical response of implant systems placed in the maxillary posterior region under various conditions of angulation, bone density and loading. The International Journal of Oral & Maxillofacial Implants 2008; 23(1):57-64.

13. Cohen M. Interdisciplinary treatment planning: principles, design, implementation. Chapter 3. Chicago: Quintessence, 2008.

14. Lazzara RJ. Immediate implant placement into extraction sites: surgical and restorative advantages. Int J Periodontics Restorative Dent 1989; 9(5):332–43.

15. Mohanad Al-Sabbagh. Implants in the Esthetic Zone. Dent Clin N Am 2006; 50: 391-407.

16. Buser D, Martin W, Belser UC. Optimizing esthetics for implant restorations in the anterior maxilla: anatomic and surgical considerations. The International Journal of Oral & Maxillofacial Implants 2004;19(Suppl):43-61.

17. Yildrium M, Fischer H, Marx R, Edelhoff D. In vivo fracture resistance of implant supported all ceramic restorations. J Prosthet Dent 2009; 90(4):325-331

18. Aramouni P, Zebouni E, Tashkandi E, Dib S, Salameh Z, Alamas K. Fracture resistance and failure location of zirconium and metallic implant abutments. Journal of Contemporary Dent Pract 2008;9(7): 41-48.

19. Kerstein RB, Radke J. A comparison of fabrication precision and mechanical reliability of two zirconia implant abutments. Int J Oral Maxillofac Implants 2008;23(6):1029-1036

20. Adatia ND, Bayne SC, Cooper LF. Fracture resistance of Yttria –Stabilized Zirconia Dental Implant Abutments. Journal of Prosthodontics 2009; 18: 17-22.

21. Nothdurft FP, Doppler KE, Erdelt KJ, Knauber AW, Pospiech PR. Fracture behavior of straight or angulated zirconia implant abutments supporting anterior single crowns. Clin Oral Invest 2011; 15: 157-163.

22. Sailer I, Sailer T, Stawarczyk B, Jung RE, Hammerle HF. In Vitro Study of the Influence of the Type of Connection on the Fracture Load of Zirconia Abutments with Internal and External Implant-Abutment Connections. The International Journal of Oral & Maxillofacial Implants 2009; 24(5):850-858

23. Wang H, Aboushelib MN, Feilzer AJ. Strength influencing variables on CAD/CAM zirconia framework. Dent Mater 2008;24: 633-638.

24. Aboushelib MN, Salameh Z. Zirconia Implant Abutment Fracture: Clinical case reports and precaution for use. The International Journal of Prosthodontics 20089;22(6): 616-619.

25. Ellakwa A, Raj T, Deeb S, Ronaghi G, Martin Fe, Klineberg I. Influence of implant abutment angulation on the fracture resistance of overlaying CAM-milled zirconia single crowns. Australian Dental Journal 2011;56:132-140.

26. Sailer I, Philipp A, Zembic A, Pjetursson BE, Hammerle CH, Zwahlen MZ. A systematic review of the performance of ceramic and metal implant abutments supporting fixed implant reconstructions. Clin Oral Impl Res 2009; 20(Suppl.4):4-31.

27. Maeda Y, Satoh T, Sogo M. In-vitro differences of stress concentrations for internal and external hex implant-abutment connections: A short communication. J Oral Rehabil 2006; 33:75–78.

28. Merz BR, Hunenbart S, Belser UC. Mechanics of the implant- abutment connection: An 8-degree taper compared to a butt joint connection. Int J Oral Maxillofac Implants 2000; 15: 519–526.

29. Turp V, Tuncelli B, Sen D, Goller G. Evaluation of hardness and fracture toughness, coupled with microstructural analysis of zirconia ceramics stored in environments with different pH values. Dental Materials Journal 2012; 31(6): 891–902.

30. Kobayashi K, Kuwajima H, Masaki T. Phase change and mechanical properties of ZrO2-Y2O3 solid electrolyte after aging. Solid State Ionics 1981; 3/4: 489-493.

31. Hirano M. Inhibition of low temperature degradation of tetragonal zirconia ceramics - a review. Br Ceram Trans J 1992;91: 139-147.

32. Piconi C, Maccauro G. Zirconia as a ceramic biomaterial. Biomaterials 1999; 20:1-25.

33. Zhang Y, Pajares A, Lawn BR. Fatigue and damage tolerance of Y-TZP ceramics in layered biomechanical systems. J Biomed Mater Res B Appl Biomater 2004; 71:166-171.

34. Chevalier J, Cales B, Drouin JM. Low-temperature aging of Y-YZP ceramics. J Am Ceram Soc 1999; 82:2150-2154.

35. Raigrodski AJ. Contemporary all-ceramic fixed partial dentures: a review. Dent Clin North Am 2004; 48:531-544.

36. Kim JW, Covel NS, Guess PC, Rekow ED, Zhang Y. Concerns of Hydrothermal Degradation in CAD/CAM Zirconia. J Dent Res 2010; 89(1):91-95.

37. Deville S, Chevalier J, Gremillard L. Influence of surface finish and residual stresses on the ageing sensitivity of biomedical grade zirconia. Biomaterials 2006; 27:2186-2192.

38. Chevalier J. What future for zirconia as a biomaterial? Biomaterials 2006; 27:534-543.

39. Proffit WR, Fields HW, Sarver DM. Contemporary Orthodontics (Fourth Edition). St. Louis. Missouri: Mosby Publication, 2000.

40. Kim H-T, Han J-S, Yang J-H, Lee J-B, Kim S-H. The effect of low temperature aging on the mechanical property & phase stability of Y-TZP ceramics. J Adv Prosthodont 2009;1: 113-117.

41. Alghazzawi TF, Lemons J, Liu P-R, Essig ME, Bartolucci AA, Janowski GM. Influence of low temperature environmental exposure on the mechanical property and structural stability of dental zirconia. Journal of Prosthodontics 2012; 21:363-369.

42. Paphangkorakit J, Osborn JW. The effect of pressure on a maximum incisal bite force in man. Archs oral Biol 1997; 42(1):11-17.

APPENDIX A

PROPERTIES OF ZIRONIA MATERIAL

zirconia material identifier	NS	NT
Used in	zirconia abutment	zirconia crown
ZrO2	92.19	91.67
Y2O3	5.6%	5.5%
HfO2	1.91%	1.83%
Al2O3	0.25%	0.05%
Others	0.05%	0.43%
Density (ρ)	6.06	6.08
Thermal expansion coefficient	$10x10^{-6}$ 25-500℃	$10x10^{-6}$ 25-500℃
Flexural strength (Mpa)	1500 Mpa	1100 Mpa
Fracture toughness (KIC)	5-6	7-8
Modulus of elasticity (GP)	210	200
Grain size	0.35	0.35
Vickers hardness (HV 10)	1200	1200
Melting point (C)	2680	2680
Shrinkage after sintering (%)	19.40-20.10	19.20-19.70

APPENDIX B

ABUTMENT SIZE MEASUREMENTS FOR ZERO DEGREE SAMPLES

NO	D, mm	M, mm	F, mm	L, mm
1	2.31	2.31	2.72	2.45
2	2.26	2.26	2.7	2.52
3	2.32	2.31	2.78	2.55
4	2.32	2.38	2.77	2.43
5	2.29	2.37	2.79	2.48
6	2.29	2.35	2.77	2.5
7	2.38	2.42	2.78	2.58
8	2.33	2.33	2.76	2.51
9	2.29	2.34	2.74	2.46
10	2.32	2.29	2.76	2.54
11	2.35	2.34	2.85	2.52
12	2.32	2.4	2.79	2.53
13	2.29	2.38	2.78	2.54
14	2.31	2.39	2.8	2.55
15	2.28	2.33	2.76	2.54
16	2.31	2.28	2.76	2.62
17	2.25	2.26	2.83	2.59
18	2.27	2.27	2.71	2.56
19	2.3	2.37	2.75	2.48
20	2.31	2.24	2.81	2.64
MEAN	2.31	2.33	2.77	2.53
SD	0.030	0.052	0.037	0.0543

Note: See figure 14 for the schematic sketch

APPENDIX C

ABUTMENT SIZE MEASUREMENTS FOR 20 ZERO FACIAL SAMPLES

NO	D, mm	M, mm	F, mm	L, mm
1	3.34	3.21	3.62	1.49
2	3.46	3.29	3.54	1.38
3	3.66	3.32	3.57	1.43
4	3.59	3.35	3.68	1.42
5	3.35	3.22	3.66	1.39
6	3.63	3.53	3.4	1.48
7	3.62	3.45	3.56	1.44
8	3.4	3.5	3.66	1.41
9	3.44	3.47	3.53	1.44
10	3.29	3.36	3.6	1.54
11	3.47	3.43	3.7	1.54
12	3.63	3.68	3.58	1.57
13	3.58	3.24	3.57	1.39
14	3.29	3.34	3.57	1.48
15	3.4	3.3	3.75	1.53
16	3.54	3.49	3.57	1.46
17	3.42	3.69	3.53	1.52
18	3.53	3.56	3.42	1.41
19	3.34	3.56	3.48	1.45
20	3.44	3.64	3.57	1.52
MEAN	3.47	3.43	3.58	1.46
SD	0.120	0.150	0.087	0.0575

Note: See figure 16 for the schematic sketch

APPENDIX D

ABUTMENT SIZE MEASUREMENTS FOR 20 DEGREE LINGUAL SAMPLES

NO	D, mm	M, mm	F, mm	L, mm
1	2.53	2.6	1.5	2.7
2	2.76	2.52	1.57	2.8
3	2.57	2.69	1.59	2.75
4	2.47	2.43	1.51	2.69
5	2.49	2.49	1.55	2.44
6	2.53	2.4	1.57	2.71
7	2.58	2.54	1.52	2.65
8	2.44	2.58	1.57	2.82
9	2.47	2.67	1.55	2.69
10	2.43	2.5	1.59	2.77
11	2.43	2.56	1.62	2.87
12	2.77	2.78	1.66	2.56
13	2.55	2.46	1.59	2.68
14	2.4	2.44	1.62	2.7
15	2.74	2.5	1.55	2.5
16	2.74	2.57	1.56	2.87
17	2.67	2.69	1.55	2.74
18	2.79	2.69	1.53	2.85
19	2.76	2.56	1.55	2.76
20	2.67	2.62	1.59	2.62
MEAN	2.59	2.56	1.57	2.71
SD	0.135	0.102	0.039	0.1153

Note: See figure 18 for the schematic sketch